Prostaglandin E Receptors in Bile Ducts of Hepatolithiasis Patients and the Pathobiological Significance for Cholangitis

JUNICHI SHODA,* TETSUYA UEDA,† TORU KAWAMOTO,§ TAKESI TODOROKI,§ TORU ASANO,* YUKIHIKO SUGIMOTO,‖ ATSUSHI ICHIKAWA,‖ TAKAYUKI MARUYAMA,¶ YUJI NIMURA,# and NAOMI TANAKA*

Departments of *Gastroenterology and §Gastrointestinal Surgery, Institute of Clinical Medicine, University of Tsukuba, Ibaraki; †Department of Pharmaceutical Research, Mitsubishi Kagaku Bio-Clinical Laboratories, Inc., Tokyo; ‖Department of Physiological Chemistry, Faculty of Pharmaceutical Sciences, University of Kyoto, Kyoto; ¶Minase Research Institute, ONO Pharmaceutical Co., Ltd., Osaka; and #First Department of Surgery, Nagoya University School of Medicine, Aichi, Japan

Background & Aims: In hepatolithiasis, chronic proliferative cholangitis may influence the progression of the disease. Prostaglandin (PG) E_2 experimentally causes morphologic changes to intrahepatic bile ducts, analogous to the changes found in cholangitis. This study was designed to gain an understanding of the involvement of PGE_2 and PGE receptor (EP) subtypes in the development of cholangitis. *Methods:* The expression levels of secretory-type group IIA phospholipase A_2 ($sPLA_2$-IIA) and cyclooxygenase (COX)-2 as well as EP subtypes were determined in the bile ducts with change of cholangitis. In in vitro experiments, growth promotion and mucin secretagogue properties of biliary epithelial cells in response to EP-selective agonists or antagonists were studied. *Results:* The messenger RNA (mRNA) level of $sPLA_2$-IIA and the protein and mRNA levels of COX-2 were significantly increased in the bile ducts of patients with hepatolithiasis compared with the levels of the bile ducts of control subjects. These changes were associated with a concomitant increase in PGE_2 and total mucin concentrations in the bile. The mRNAs of EP subtypes EP_2, EP_3, and EP_4 but not EP_1 were amplified in the bile ducts. Treatment with an EP_4-selective agonist (ONO-AE1-329) caused a dose-dependent increase in DNA synthesis, colony number, and mucin secretion in the cells. Conversely, treatment with an EP_4-selective antagonist (ONO-AE3-208) abolished the biological effects of PGE_2 on the cells. *Conclusions:* In hepatolithiasis, an enhanced synthesis of $sPLA_2$-/COX-2–derived PGE_2 and its actions mediated via the EP_4 receptor in the bile ducts may be of pathobiological significance for chronic proliferative cholangitis.

Hepatolithiasis is prevalent in the Far East, including Japan, but is extremely rare in western countries.[1,2] The distinctive feature is an intractable course requiring multiple operative interventions with frequent recurrence. This is in sharp contrast to ordinary cholelithiasis, in which stones are usually found in the gallbladder and/or extrahepatic bile ducts mostly consisting of cholesterol stones or black pigment stones. Most stones in hepatolithiasis appear as brown pigment stones (calcium bilirubinate stones),[3] which differ from cholesterol and black pigment stones in their composition[4] and etiology.[5,6] Bacterial infection and bile stasis are believed to be of importance for the pathogenesis of the disease.[7,8]

The main morphologic feature of stone-containing bile ducts in hepatolithiasis is chronic proliferative cholangitis,[9,10] a condition in which intramural and extramural peribiliary glands proliferate to a marked degree and in which the lining epithelia are hyperplastic. Chronic inflammation precedes bile duct deformations, that is, strictures and/or dilatation, both of which in turn may cause bile static alterations of biliary flow owing to an uneven inner surface of the affected bile ducts. Moreover, most proliferating glands have mucin-producing activity.[9] Excessive amounts of mucin secreted into the inner surfaces of the ducts may provide a microenvironment that initiates a nidus for stones and also cause stones to expand by altering biliary flow in bile ducts.

In animal experiments, administration of a prostaglandin (PG) E_2 analogue in the setting of bile stasis and bacterial infection has been shown to enhance proliferation of mucus-producing glandular elements and hyperplasia of the surface bile duct epithelia,[11] similar to findings of chronic proliferative cholangitis in human hepatolithiasis.[9,10]

Abbreviations used in this paper: cAMP, adenosine 3′,5′-cyclic monophosphate; COX, cyclooxygenase; EP, prostaglandin E receptor; mRNA, messenger RNA; PG, prostaglandin; PLA_2, phospholipase A_2; RT-PCR, reverse-transcription polymerase chain reaction; $sPLA_2$-IIA, secretory-type group IIA phospholipase A_2.

1542-3565/03/$30.00
doi:10.1016/S1542-3565(03)00133-2

Biological activity of PGE_2[12–14] is attributed to 4 specific G protein–coupled PGE receptor (EP) subtypes. Recent studies have shown that EP messenger RNAs (mRNAs) are distributed throughout the gastrointestinal tract,[15,16] and the biological effect of PGE_2 in gastrointestinal tissues involves signaling via several EP subtypes. The pathobiological effects of PGE_2 via EP subtypes on biliary epithelia and glands may be involved in their phenotypic changes under the condition of chronic proliferative cholangitis.

A series of our studies[17,18] has shown that induction of secretory-type phospholipase A_2 ($sPLA_2$) isoforms causatively potentiates arachidonate metabolism, yielding a large amount of PGE_2, and thereby propagates bile duct inflammation (cholangitis) in hepatolithiasis.

In this study, we aimed to achieve a better understanding of the pathogenesis of hepatolithiasis with special reference to involvement of PGE_2 and EP subtypes in chronic proliferative cholangitis. We determined the expression levels of inflammatory enzymes in the arachidonate cascade, $sPLA_2$ isoforms, and cyclooxygenases (COXs) as well as EP subtypes in the bile ducts. Furthermore, in in vitro experiments, both growth promotion and mucin secretagogue properties of biliary epithelial cells in response to treatment with specific agonists or antagonists of EP subtypes as well as PGE_2 were studied.

Patients and Methods

Patients

The study was performed from 1998 to 2000 in cooperation with the study group for the National Survey Project of Intrahepatic Calculi organized by the Ministry of Health and Welfare of Japan (Director, Professor Yuji Nimura). The protocol for the present study was approved by the official committee of the survey. Study procedures were in accordance with the ethical standards of the Helsinki Declaration. Written informed consent was obtained for each patient.

Fourteen patients with primary hepatolithiasis (6 men and 8 women) with only one of the 2 hepatic lobes affected by stones (2 patients with affected right lobes and 12 patients with affected left lobes) were included in this study (Table 1). The classification of hepatolithiasis was based on the criteria described by Nakayama.[19] The gallstones were classified according to the proceedings of the first National Institutes of Health International Workshop on Pigment Gallstone Disease.[20] In addition, 12 patients with so-called primary common bile duct stones that were accompanied by neither intrahepatic nor gallbladder stones, 18 patients with gallbladder stones that were accompanied by neither intrahepatic nor common bile duct stones, and 8 patients with metastatic colon carcinoma in the liver were included.

Table 1. Data on Patients With Hepatolithiasis

Patients	
n	14
Sex (M/F)	6/8
Mean age, *yr* (range)	64 (48–72)
Stone location	
Intrahepatic bile duct only	14
Intrahepatic and extrahepatic ducts	0
Right lobe only	2
Left and right lobes	0
Left lobe only	12
Bile duct	
Stricture	
+	13
−	1
Dilation	
+	14
−	0
Gallbladder stones	
+	3
−	11
Liver atrophy and fibrosis[a]	
+	4
−	10

NOTE. The above classification of stones is based on the criteria described by Nakayama.[19]
[a]Findings based on macroscopic examination.

Gallstones

The gallstone specimens obtained at surgery were classified by visual inspection and infrared analysis.[21] All of the gallstones were classified as brown pigment stones.

Bile

Ductal bile was obtained from the stone-containing hepatic ducts in patients with hepatolithiasis, with particular care taken to avoid contamination with blood. Ductal bile was also obtained from the common bile ducts of 12 patients with primary common bile duct stones and from the common bile ducts of 18 patients with gallbladder stones. All specimens were subject to bacterial examinations for aerobes and anaerobes. Eight of the 14 specimens drained from affected ducts but none of the 4 specimens from unaffected ducts of 14 patients with intrahepatic brown pigment stones were positive for bacteria. Cultures of the bile specimens were positive for both aerobes and anaerobes. The bacteria isolated were as follows: *Escherichia coli* (7 bile specimens), *Klebsiella* spp. (5), *Enterobacter* spp. (4), *Streptococcus* (3), *Citrobacter* spp. (3), and *Bacteroides* spp. (3). In addition, 7 of the 12 specimens from the common bile duct of 12 patients with primary common bile duct stones but none of the 18 specimens from the common bile duct of 18 patients with gallbladder cholesterol stones were positive for bacteria.

Bile Ducts

Surgically resected hepatic segments from patients with hepatolithiasis were opened and then sent for histologic examination. Histologic examination of the stone-containing

bile ducts in the hepatic segments represented the typical features of chronic proliferative cholangitis.[9,10] Small parts of the resected specimens of stone-containing bile ducts with chronic proliferative cholangitis (affected bile ducts) and those of intact bile ducts (unaffected bile ducts) were immediately washed with distilled water, frozen in liquid nitrogen, and stored at −80°C until analysis. In addition, the intact intrahepatic bile duct specimens obtained from resected hepatic segments were obtained at surgery from patients with metastatic colon carcinoma.

$sPLA_2$-IIA Assay

The protein mass of $sPLA_2$-IIA levels in ductal bile was immunoradiometrically assayed as described previously.[22] Assay kits were kindly supplied by the Pharmaceuticals Research & Development Division of Shionogi & Co., Ltd. (Osaka, Japan). All assays were performed in triplicate.

Phospholipase A_2 Enzyme Activity

Phospholipase A_2 (PLA_2) enzyme activity was determined as described previously.[23] Briefly, the assay was performed using 1-palmitoyl-2-oleoyl-*sn*-glycero-3-phosphoglycerol as a substrate. Fatty acids released by PLA_2 were labeled with 9-anthryldiazomethane, and the derivatized fatty acids were separated by high-performance liquid chromatography.

PGE_2 Assay

PGE_2 levels in bile duct tissues and ductal bile were determined by a highly specific radioimmunoassay (anti-PGE_2 antibody; Amersham, London, England) according to the method described previously.[24] The final results are expressed as picograms PGE_2 per milliliter.

Mucin Assay

Mucin concentration in ductal bile was determined as described by Miquel et al.[25] Briefly, a specimen was diluted 1:1 (vol/vol) with a 0.1 mol/L Tris-HCl buffer (pH 7.5). The diluted specimen was gently shaken for 24 hours at 4°C and then centrifuged at 12,000*g* for 10 minutes. The supernatant was subsequently fractionated using Sepharose 4B-Cl gel chromatography (35 × 1-cm column; Pharmacia, Uppsala, Sweden). Mucin eluted in the void volume. Mucin concentration was determined using a fluorometric assay.[26]

Immunostaining of COX-2

Immunostaining of COX-2 was performed by the avidin-biotin complex technique using a Vectastain Elite ABC kit (Vector Laboratories, Burlingame, CA) as described recently.[27] Formalin-fixed, paraffin-embedded specimens were used. Evaluation of the sections was performed by a single pathologist who was blinded to the clinical characteristics; the COX-2 immunostaining was evaluated in terms of the intensity and positive rate of the immunostaining as described previously.[27] The intensity was defined by comparing the intensity in smooth muscles or vascular endothelia as internal built-in controls.

RNA Isolation and Complementary DNA Synthesis

Total RNA was isolated using TRIzol reagent by the modified method as described by Chomczynski and Sacchi.[28] First-strand complementary DNAs were synthesized from total RNA with Moloney murine leukemia virus reverse transcriptase by the random primer method.

Reverse-Transcription Polymerase Chain Reaction

Semiquantitative reverse-transcription polymerase chain reaction (RT-PCR) was performed using a DNA Thermal Cycler (model PJ 2000; Applied Biosystems, Inc., Foster City, CA). PCR was subjected to each cycle (glyceraldehyde-3-phosphate dehydrogenase, 20; COX-1, 30; COX-2, 30; $sPLA_2$-IIA, 35; EP_1, 35; EP_2, 35; EP_3, 35; EP_4, 35) at 94°C for 1 minute, at 55°C for 2 minutes, and at 72°C for 2 minutes. Aliquots of the reaction mixture were electrophoresed on a 2% agarose gel. PCR primers were designed from complementary DNA sequences for human COX-1,[29] COX-2,[30] $sPLA_2$-IIA,[31] EP_1,[32] EP_2,[33] EP_3,[34] and EP_4[35] and then synthesized using an Applied Biosystems DNA synthesizer (model 392; Applied Biosystems., Inc.) as follows: glyceraldehyde-3-phosphate dehydrogenase, sense 5′-GAACGGGAAGCTCACTGGCATGGC-3′, antisense, 5′-TGAGGTCCACCACCCTGTTGCTG-3′; COX-1, sense 5′-CTTGACCGCTACCAGTGTGA-3′, antisense 5′-AGAGGGCAGAATACGAGTGT-3′; COX-2, sense, 5′-AAGCCTTCTCTAACCTCTCC-3′, antisense 5′-TAAGCACATCGCATACTCTG-3′; $sPLA_2$-IIA, sense 5′-ACCATGAAGACCCTCCTACTG-3′, antisense 5′-GAAGAGGGGACTCAGCAACG-3′; EP_1, sense 5′-CGCGCTGCCCATCTTCTCCAT-3′, antisense 5′-CCCAGGCCGATGAAGCACCAC-3′; EP_2, sense 5′-GCTGCTGCTTCTCATTGTCTCG-3′, antisense 5′-TCCGACAACAGAGGACTGAACG-3′; EP_3, sense 5′-GGCACGTGGTGCTTCATC-3′, antisense 5′-GGGTCCAGGATCTGGTTC-3′; EP_4, sense 5′-ATCTTACTCATTGCCACC-3′, antisense 5′-TCTATTGCTTTACTGAGCAC-3′. Plasmid vectors into which each objective coding region of human COX-1,[29] COX-2,[30] $sPLA_2$-IIA,[31] EP_1,[32] EP_2,[33] EP_3,[34] and EP_4[35] had already been inserted were used as positive controls for the RT-PCR. In each experiment, RT-PCR was performed in triplicate. In the semiquantitative assessment, the amounts of fluorescence intensity were measured using a FluorImager (Molecular Dynamics, Sunnyvale, CA). The data were expressed relative to the amount of glyceraldehyde-3-phosphate dehydrogenase mRNA present in each specimen and then averaged. The semiquantitative measurement of RT-PCR was assessed using varying amounts of template RNA obtained from the bile duct specimens. The density of the band of the PCR product was observed to increase proportionately with template RNA for each PCR reaction. Linearity between the template RNA amount and PCR product was obtained when complementary DNA products reverse transcribed using total RNA of <100 ng were amplified at 35 cycles.

Synthesis of Complementary RNA Probes of EP Subtypes

Riboprobes were synthesized from plasmid vectors as described previously.[36] These plasmids were linearized and antisense RNA probes were transcribed with RNA polymerase in the presence of cytidine 5′-(α-thio)triphosphate [^{35}S] to a specific activity of 1×10^9 cpm/μg.

In Situ Hybridization of EP Subtypes

In situ hybridization was performed using 8-μm-thick frozen sections as described recently.[36]

Hybridization was performed in a buffer containing 50% formamide, 2× standard saline citrate, 10 mmol/L Tris-HCl (pH 7.5), 1× Denhardt's solution, 10% dextran sulfate, 0.2% sodium dodecyl sulfate, 100 mmol/L dithiothreitol, 500 μg/mL sheared single-stranded salmon sperm DNA, and 250 μg/mL yeast tRNA. Riboprobes were added to the hybridization buffer at 7×10^4 cpm/μL. The hybridization solution was applied to the slides, which were then covered with a coverslip and sealed by rubber cement. After incubation at 60°C for 5 hours, the slides were immersed in 2× SCC to remove the coverslips and then washed for 1 hour by warming in 2× SCC and 10 mmol/L β-mercaptoethanol. The sections were then treated with 20 μg/mL ribonuclease A in 0.5 mol/L NaCl, 10 mmol/L Tris-HCl (pH 7.5), and 1 mmol/L ethylenediaminetetraacetic acid, followed by an additional wash in 0.1× standard saline citrate at 60°C for 1 hour. After dehydration, the slides were dipped in NTB-2 emulsion (Eastman Kodak, Rochester, NY) diluted 1:1 with distilled water. After exposure for 4 weeks at 4°C, the dipped slides were developed in COPINAL (FujiFilm, Tokyo, Japan), diluted 1:2 in distilled water, fixed, and counterstained with H&E.

Cell Lines and Culture Conditions

Mz-ChA-1 and Mz-ChA-2, gallbladder adenocarcinoma cell lines,[37] and Sk-ChA-1, a bile duct adenocarcinoma cell line,[37] were obtained from Dr. A. Knuth (Johaness-Gutenberg University, Mainz, Germany). TGBC-1 and TGBC-2, gallbladder adenocarcinoma cell lines,[38] were obtained from Dr. T. Todoroki (University of Tsukuba, Ibaraki, Japan). The cells were maintained in Dulbecco's modified Eagle medium that contained 10% heat-inactivated fetal calf serum (Hyclone Laboratories, Inc., Logan, UT) in a humidified atmosphere with 5% carbon dioxide at 37°C. Northern blot and immunoblot of COX-2 in cell protein lysates was performed in the same manner as described previously.[36] PGE_2 production in the cells was determined by measuring PGE_2 concentration in the media from the cells with and without 50 μmol/L arachidonate treatment. The PGE_2 concentration 6 hours after the addition of arachidonate was assayed in triplicate by a radioimmunoassay in the same manner as described previously.

DNA Synthesis Assay

The Mz-ChA-2 cells were grown in complete Dulbecco's modified Eagle medium supplemented with 10% fetal calf serum for 24 hours and then in serum-free medium supplemented with test reagents. An EP_2-selective agonist (ONO-AE1-259[39]; Ono Pharmaceutical Co., Ltd., Osaka, Japan), EP_3-selective agonist (ONO-AE-248[39]), and EP_4-selective agonist (ONO-AE1-329[39]) at a concentration of 0.01, 0.1, 1, or 10 μmol/L or PGE_2 (Cayman Chemical Co., Ann Arbor, MI) at a concentration of 1 μmol/L was added daily to selected cells, and the medium was replaced every day. An EP_4-selective antagonist (ONO-AE3-208[40]) at a concentration of 0.01, 0.1, 1, or 10 μmol/L and 1 μmol/L of PGE_2 were also added daily to the cells. After incubation with the test reagents for 48 hours, the culture medium was removed and the cells were washed 3 times with phosphate-buffered saline and cultured in fresh medium containing 1 μCi/mL [methyl-^{3}H]thymidine 5′-triphosphate (ICN Biomedicals, Inc., Costa Mesa, CA) for another 6 hours. The radioactivity of incorporated [^{3}H]thymidine in the resulting cell pellets was counted by liquid scintillation. In each experiment, the assay was performed in quadruplicate. Results are expressed as a percentage of the maximal incorporation in nontreated cells.

Colony Formation Assay

The colony number of Mz-ChA-2 cells was counted according to the method described previously[41] with minor modifications. Briefly, Mz-ChA-2 cells were plated in a 10-cm cell culture disk at a density of 1000 cells/dish with Dulbecco's modified Eagle medium containing 10% fetal calf serum. ONO-AE1-259, ONO-AE-248, ONO-AE1-329, or PGE_2 was added daily to selected cells in the same way as described previously, and the medium was replaced every day. ONO-AE3-208 and PGE_2 were added daily to the cells in the same way as described previously. The cells were incubated for 14 days, and then the colonies were visualized by staining with 0.2% methylene blue and counted manually. In each experiment, the assay was performed in quadruplicate.

Mucin Secretion Assay

The mucin secretion assay was performed as described previously.[42] Mz-ChA-2 cells were labeled overnight with 1 μCi/well [^{3}H]*N*-acetyl-D-glucosamine in the medium described previously. The cells were then washed with phosphate-buffered saline (pH 7.4) and subsequently with serum-free medium to remove unincorporated label. Next, 1 mL of serum-free medium containing ONO-AE1-259, ONO-AE-248, ONO-AE1-329, or PGE_2 at the same concentrations as those used before was added to the well. In another experiment, 1 mL of serum-free medium containing ONO-AE3-208 and PGE_2 at the same concentrations as those used before was added to the wells. After incubation with the test reagents for 6 hours, 0.5 mL of medium was harvested from each well and centrifuged at 500*g* for 10 minutes to pellet released cells. A specimen of the supernatant was used for the assay. Parts of the cell pellet were used for protein determination using a bicinchoninic acid protein assay kit (Pierce, Rockford, IL). Results are expressed as percentage of control in counts per minute per milligram protein.

Adenosine 3',5'-Cyclic Monophosphate Assay

Mz-ChA-2 cells were washed with phosphate-buffered saline (pH 7.4) and subsequently with serum-free medium. A total of 0.5 mL of serum-free medium containing ONO-AE1-259, ONO-AE-248, ONO-AE1-329, or PGE_2 at the same concentrations as those used previously was added to the cells in the wells. In another experiment, 0.5 mL of serum-free medium containing ONO-AE3-208 and PGE_2 at the same concentrations as those used previously was added to the cells. After incubation with the test reagents for 5 minutes, the cells were quickly dissolved in a lysis buffer and the intracellular adenosine 3',5'-cyclic monophosphate (cAMP) concentration in the cell lysates was measured using a cAMP enzyme immunoassay kit (BioRad, Hercules, CA). The protein concentration was determined using a bicinchoninic acid protein assay kit. Results are expressed as picomoles cAMP per milligram protein.

Statistics

Values are given as means ± SEM. Means of 2 groups were compared with the Mann-Whitney rank sum U test (2-tailed test), and multiple comparisons were performed by analysis of variance. A 2-sided χ^2 test was used for comparison of clinicopathologic data between groups. $P < 0.05$ was defined as statistically significant.

Results

Immunostaining of COX-2 in Intrahepatic Bile Ducts

Immunostaining of COX-2 was observed in the epithelia of normal intrahepatic bile ducts (Figure 1*A*). The intensity of the immunostaining, which was as weak as that in smooth muscles or vascular endothelia of the vessels used as internal controls (Figure 1*B*), was mostly grade 1 intensity. However, in the bile ducts with chronic proliferative cholangitis from patients with hepatolithiasis, intense immunostaining of COX-2 (grade 2 intensity) was observed in the intramural proliferating glandular elements (Figure 1*B*), including mucus glands (Figure 1*C*) of the bile ducts as well as in the lining epithelia with hyperplastic change (Figure 1*D*). In the lining epithelia, although the positive rate of COX-2 was 100% both in normal intrahepatic bile ducts and those with chronic proliferative cholangitis, COX-2 immunostaining of grade 2 intensity was observed more frequently in the latter group than in the former group (Table 2). COX-2 immunostaining of grade 2 intensity was also observed at a high frequency in the proliferating glandular elements (Table 2).

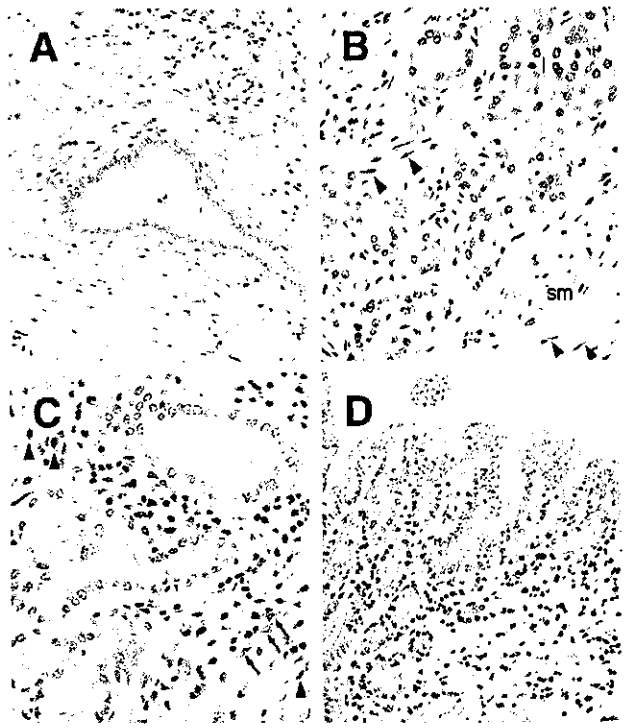

Figure 1. Grading intensity of immunostaining of COX-2 in bile ducts. (*A*) A normal intrahepatic bile duct in a specimen of resected liver segments from a patient who underwent hepatectomy because of metastatic colon carcinoma. Weak immunostaining of COX-2 (grade 1 intensity) was observed in the epithelia. (*B*) Proliferated intramural glands of the bile duct affected by intrahepatic stones in a specimen of resected liver segments from a case of hepatolithiasis. Intense immunostaining of COX-2 (grade 2 intensity) was observed in the glandular epithelia. Weak immunostaining of COX-2 (grade 1 intensity) was observed in the smooth muscles or vascular endothelia (as internal built-in controls) of the vessels. (*C*) Proliferated intramural glands including mucus of the bile duct affected by intrahepatic stones in a specimen of resected liver segments from a case of hepatolithiasis. Intense immunostaining of COX-2 (grade 2 intensity) was observed in the mucus glands. (*D*) Hyperplastic epithelia of the bile duct affected by intrahepatic stones in a specimen of resected liver segments from a case of hepatolithiasis. Intense immunostaining of COX-2 (grade 2 intensity) was observed in the epithelia. Original magnification: *A*, *B*, and *D*, 66×; *C*, 132×.

Tissue mRNA Levels of $sPLA_2$-IIA, COX-1, COX-2, and EP_{2-4} Subtypes and Tissue Concentration of PGE_2 in Intrahepatic Bile Ducts

Figure 2 shows the PCR-assisted amplifications of $sPLA_2$-IIA, COX-1, COX-2, and EP_{2-4} subtype mRNAs in the tissue specimens of bile ducts. The mRNA level of COX-2 was significantly higher in specimens of affected bile ducts from 14 patients with hepatolithiasis and specimens of unaffected bile ducts than in specimens of normal bile ducts as shown in Table 3, whereas the level of COX-1 mRNA was not significantly different in the specimens. The increased COX-2 mRNA levels in the

Table 2. Immunohistochemical Expression of COX-2 in the Lining Epithelia and Glandular Elements of Bile Ducts

	Normal bile duct (8)				Hepatolithiasis (14)			
		Grading intensity				Grading intensity		
	Positive rate	0	1	2	Positive rate	0	1	2
Lining epithelia	8/8	0	6	2	14/14	0	0	14[a]
Glandular elements	ND		ND		14/14	0	1	13

NOTE. Immunostaining of COX-2 was evaluated in terms of the positive rate and intensity as described in Patients and Methods. Lining epithelia, glandular elements, and stroma of the bile ducts were divided into 2 groups based on the intensity of staining of COX-2: one group of cases in which the intensity was graded as 0 or 1, and the other group of cases in which the intensity was graded as 2. Comparisons of the intensity were made between 8 cases of normal bile ducts and 14 cases of bile ducts affected by gallstones in hepatolithiasis.
ND, not determined.
[a]$P < 0.01$, significantly different between the normal bile duct group and the hepatolithiasis group.

bile ducts of patients with hepatolithiasis are consistent with the results of immunostaining of COX-2 (Figure 1). Of the $sPLA_2$ isoforms, the mRNA of $sPLA_2$-IIA was strongly expressed in specimens of affected bile ducts but only weakly expressed in specimens of normal bile ducts.

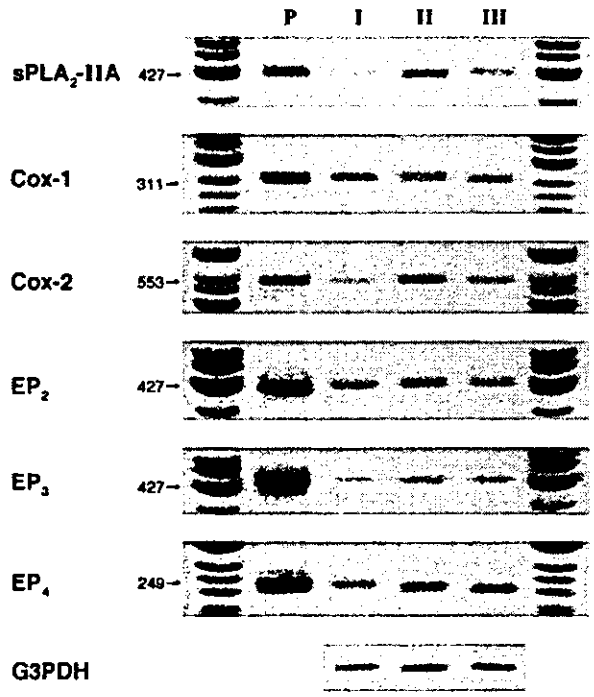

Figure 2. PCR-assisted amplifications of mRNAs of $sPLA_2$-IIA, COX-1, COX-2, EP_2, EP_3, and EP_4 in bile duct tissues. Plasmid vectors into which each objective coding region of human COX-1,[30] COX-2,[31] $sPLA_2$-IIA,[32] EP_2,[34] EP_3,[35] and EP_4[36] had already been inserted were used as positive controls. *Lane P*, positive controls; *lane I*, a specimen of normal bile duct; *lane II*, a specimen of bile duct affected by intrahepatic stones; *lane III*, a specimen of unaffected bile duct. The abundance of glyceraldehyde-3-phosphate dehydrogenase mRNA was determined as an internal standard. The PCR products were 449 base pairs in size for $sPLA_2$-IIA, 309 base pairs for COX-1, 531 base pairs for COX-2, 392 base pairs for EP_2, 416 base pairs for EP_3, 212 base pairs for EP_4, and 311 base pairs for glyceraldehyde-3-phosphate dehydrogenase.

Similar to the COX-2 expression levels, the mRNA level of $sPLA_2$-IIA was significantly higher in specimens of affected bile ducts than in specimens of normal bile ducts. The magnitude of the increases in COX-2 and $sPLA_2$-IIA mRNA levels was greater in the affected than in the unaffected bile ducts (Table 3).

The tissue concentrations of PGE_2 were significantly increased in specimens of affected bile ducts from patients with hepatolithiasis and in specimens of unaffected bile ducts than in specimens of normal bile ducts (Table 3).

Of the EP subtypes, the mRNAs of EP_2, EP_3, and EP_4, but not the mRNA of EP_1, were amplified in the tissue specimens of bile ducts (Figure 2). The mRNA level of each of the EP_{2-4} subtypes determined by semiquantitative assessment was significantly higher in specimens of affected bile ducts from patients with hepatolithiasis than in specimens from normal bile ducts (Table 3).

In Situ Hybridization of mRNAs of EP Subtypes in Intrahepatic Bile Ducts

In the intrahepatic bile ducts with chronic proliferative cholangitis, mRNAs of EP subtypes EP_2, EP_3, and EP_4 were predominantly expressed mostly in the proliferating glandular elements (Figure 3*A–C*), including mucus glands (Figure 3*D*), and in the lining epithelia with hyperplastic change (Figure 3*E*). However, in the normal intrahepatic bile ducts, the mRNAs of these EP subtypes were expressed only weakly in the lining epithelia (data not shown). The mRNA localization of EP subtypes shown by in situ hybridization in the bile ducts of patients with hepatolithiasis supports the results of the increased mRNA levels of EP subtypes shown by RT-PCR analysis.

PLA_2 Enzyme Activity and $sPLA_2$-IIA, PGE_2, and Mucin Concentrations in Ductal Bile

PLA_2 enzyme activity in the ductal bile was significantly higher in patients with common bile duct

Table 3. Steady-state mRNA Levels of $sPLA_2$-IIA, COX-1, COX-2, EP_2, EP_3, and EP_4 and Tissue Concentration of PGE_2 in the Bile Ducts of Control Subjects and Patients With Hepatolithiasis

		Hepatolithiasis	
	Controls IHBD⁻ (n = 12)	IHBD⁺ (n = 14)	IHBD⁻ (n = 8)
% Glyceraldehyde-3-phosphate dehydrogenase			
$sPLA_2$-IIA	33 ± 5	215 ± 20[a,b]	101 ± 5
COX-1	128 ± 10	106 ± 9	110 ± 9
COX-2	52 ± 3	161 ± 14[a,b]	93 ± 4[a]
EP_2	75 ± 8	185 ± 13[a,b]	105 ± 5
EP_3	39 ± 7	99 ± 6[a,b]	72 ± 5[a]
EP_4	91 ± 6	189 ± 20[a,b]	115 ± 8
pg/mg protein			
PGE_2	75 ± 6	2820 ± 349[a,b]	336 ± 37

NOTE. Values are given as means ± SEM. IHBD, intrahepatic bile ducts; +, affected by gallstones; −, unaffected by gallstones.
[a]$P < 0.01$, significantly different from the IHBD of control subjects.
[b]$P < 0.01$, significantly different from the unaffected IHBD of patients with hepatolithiasis.

stones and in patients with hepatolithiasis than in patients with gallbladder stones (Table 4). Paralleling the increased PLA_2 activity, the $sPLA_2$-IIA levels were significantly higher in bile from patients with common bile duct stones and in bile from affected hepatic ducts of patients with hepatolithiasis than in bile from bile ducts of patients with gallbladder stones (Table 4).

The PGE_2 concentrations were significantly higher in bile from patients with common bile duct stones and in bile from affected ducts of patients with hepatolithiasis than in bile from patients with gallbladder stones (Table 4).

Furthermore, the total mucin concentrations in bile were significantly higher in patients with common bile duct stones and in patients with hepatolithiasis than in patients with gallbladder stones (Table 4).

Effects of EP_{2-4}-Selective Agonists or EP_4-Selective Antagonist on Colony Formation and Mucin Secretion in Biliary Epithelial Cells

COX-2 protein and mRNA were expressed strongly in TGBC-1, TGBC-2, and Mz-ChA-1 cells but not in Mz-ChA-2 and Sk-ChA-1 cells (Figure 4*A*). TGBC-1, TGBC-2, and Mz-ChA-1 cells produced significant amounts of PGE_2 in response to treatment with 50 μmol/L arachidonate for 6 hours, whereas Mz-ChA-2 and Sk-ChA-1 cells produced only trace amounts (Figure

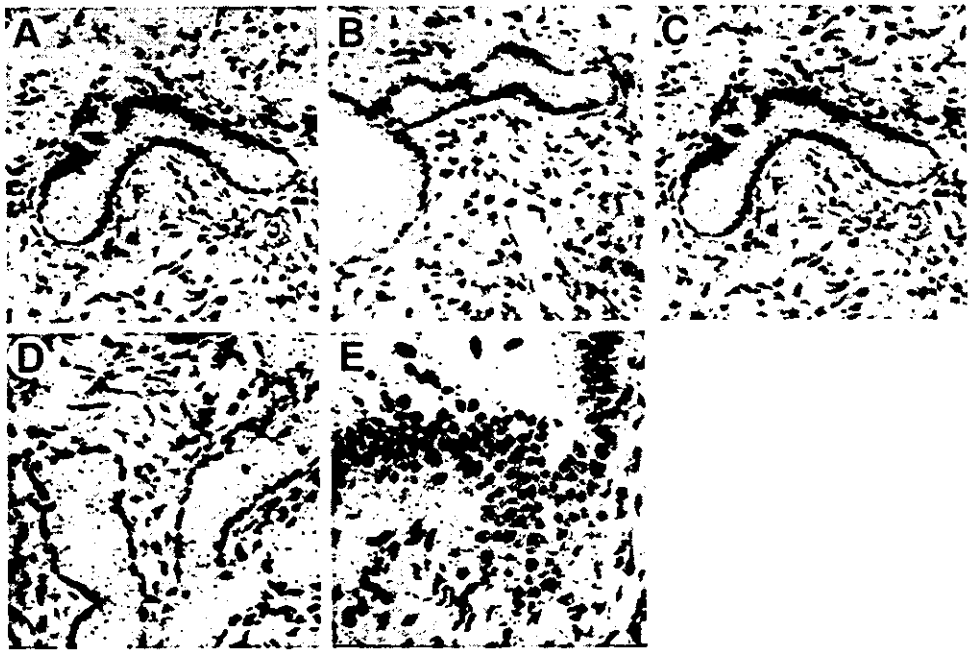

Figure 3. In situ hybridization of EP_{2-4} in the bile duct affected by intrahepatic stones in a specimen of resected liver segments from a case of hepatolithiasis. The mRNAs of (*A*) EP_2, (*B*) EP_3, and (*C*) EP_4 subtypes are diffusely expressed in the epithelia of proliferated intramural glands (original magnification 200×).

Table 4. Comparison of Ductal Bile of Patients With Gallbladder Stones, Those With Common Bile Duct Stones, and Those With Hepatolithiasis

	Gallbladder stones CBD⁻ (n = 18)	Common bile duct stones CBD⁺ (n = 12)	Hepatolithiasis IHBD⁺ (n = 14)
$sPLA_2$ activity (*nmol/min/mL*)	2.1 ± 0.1	7.5 ± 0.6[a]	14.0 ± 2.4[a]
$sPLA_2$-IIA concentration (*ng/dL*)	53 ± 5	109 ± 18[a]	348 ± 51[a]
PGE_2 concentration (*pg/mL*)	554 ± 39	1612 ± 210[a]	2,689 ± 178[a]
Total mucin concentration (*mg/mL*)	0.11 ± 0.01	0.29 ± 0.04[a]	0.46 ± 0.03[a]

NOTE. Values are given as means ± SEM. CBD, bile from common bile ducts; IHBD, bile from intrahepatic bile ducts; +, affected by gallstones; −, unaffected by gallstones.
[a]$P < 0.01$, significantly different from patients with gallbladder stones.

4*A*). The mRNAs of EP_2, EP_3, and EP_4 were amplified in Mz-ChA-2 cells (Figure 4*B*), whereas EP_1 mRNA was not detected. In in situ hybridization, EP_{2-4} mRNAs were diffusely and strongly expressed in the cells (Figure 4*C*).

To elucidate the involvement of PGE_2 and EP subtypes to chronic proliferative cholangitis, we studied the biological effect of PGE_2 on biliary epithelial cells via EP subtypes by evaluating the effects of EP_{2-4}-selective agonists or PGE_2 treatment on DNA synthesis, colony formation, and mucin secretion in a monolayer culture of Mz-ChA-2 cells (Table 5). Mz-ChA-2 cells were used for the present experiments because endogenous production of PGE_2 was observed to be very low in the cells and, thus, the signaling pathway via EP_{2-4} may be less activated. A dose-dependent increase in DNA synthesis and in colony number following treatment with an EP_4-selective agonist (ONO-AE1-329) was observed in the cells. The EP_4 agonist and PGE_2 at concentrations of 1 μmol/L caused approximately 1.9- and 2.2-fold increases in DNA synthesis and approximately 1.9- and 1.8-fold increases in colony number, respectively (Table 5). Furthermore, a dose-dependent increase in the amount of mucin secretion following treatment with the EP_4 agonist was also observed in the cells. The EP_4 agonist and PGE_2 at concentrations of 1 μmol/L caused approximately 1.6- and 1.8-fold increases in the amount of mucin secretion (Table 5).

To further confirm that PGE_2 mediates phenotypic changes in biliary epithelial cells by acting on the EP_4 receptor, we also examined the inhibitory effect of an EP_4-selective antagonist (ONO-AE3-208) on Mz-ChA-2 cells. Elevated values of DNA synthesis, colony number, and amount of mucin secretion induced by treatment with 1 μmol/L PGE_2 were dose-dependently suppressed by simultaneous addition of the EP_4 antagonist in the cells (Table 5).

Effects of EP_{2-4}-Selective Agonists or EP_4-Selective Antagonist on Intracellular cAMP Concentrations in Biliary Epithelial Cells

Changes in intracellular cAMP concentrations in Mz-ChA-2 cells in response to treatment with EP_{2-4}-selective agonists, EP_4-selective antagonist, or PGE_2 were determined. The results are summarized in Table 6. Treatment with the EP_4 agonist caused a dose-dependent increase in intracellular cAMP, with maximal production occurring at a concentration of 1 μmol/L (12-fold increase). On the other hand, treatment with the EP_4 antagonist abolished the PGE_2-evoked increase in cAMP production in the cells, with maximal inhibition occurring at a concentration of 1 μmol/L. Treatment with 1 μmol/L of the EP_2 agonist caused a slight but significant increase in cAMP production in the cells. Treatment with the EP_3 agonist caused no inhibition in intracellular cAMP in the cells. Taken together, these results clearly show that PGE_2 interacts at the EP_4 receptor of the cells to induce growth promotion or cAMP-dependent mucin exocytosis.

Discussion

The pathogenetic factors responsible for the development of hepatolithiasis have not been fully elucidated. Chronic proliferative cholangitis is one of the main factors responsible for the initiation as well as progression of the disease.[9,10]

The events initiating chronic proliferative cholangitis are not fully addressed but are believed to be the acute inflammation of bile duct epithelia caused by infective organisms via the portal vein or alterations of bile components; lipopolysaccharide in bacterial species or a larger mass of cholesterol crystals in the cholesterol supersaturated bile, due to abnormal cholesterol and bile acid metabolism in the liver,[43,44] act as proinflammatory agents and trigger inflammatory responses in bile duct

epithelia. The alterations of bile components may potentiate arachidonate metabolism not only in bile duct epithelia affected by gallstones but also in intact duct epithelia in the liver of patients with hepatolithiasis. In hepatolithiasis, the enhanced arachidonate metabolism and EP-mediated inflammatory responses in the bile duct wall may be described as we previously reported for cholesterol gallstones in the gallbladder.[17]

COX-2 is the rate-limiting enzyme for PG synthesis. Results of immunostaining and RT-PCR analysis performed using specimens of stone-containing bile ducts with chronic proliferative cholangitis (affected bile ducts) showed increased levels of COX-2 protein and mRNA in the proliferating glandular elements, including mucus glands, and the lining epithelia with hyperplastic change (Figures 1 and 2). In in vitro experiments, there seemed to be a significant increase in PGE_2 production in the COX-2–expressing biliary epithelial cells in response to arachidonate treatment (Figure 4). Therefore, in affected bile ducts, the glands or epithelia could be a potent source of PGE_2. Because PGE_2 stimulates cell proliferation,[41] inhibits apoptosis,[45] and induces growth factor–mediated angiogenesis,[46] PGE_2 produced there in situ through its action via EP subtypes may play an important role in the pathobiology of cholangitis, such as proliferation of the epithelia and glandular elements and/or formation and maintenance of the stroma and vessel structure.

In conjunction with the elevated expression level of COX-2, the high expression level of $sPLA_2$-IIA mRNA in bile ducts could provide arachidonate, a substrate for COX-2, and lead to increased PGE_2 production. It is also possible that $sPLA_2$ isoforms themselves are directly related to the pathobiology of cholangitis, because $sPLA_2$ receptor-mediated biological responses include stimulation of cellular proliferation (DNA synthesis).[47]

As found in several studies,[48–50] the biological effect of PGE_2 in gastrointestinal tissues involves signaling via several EP subtypes. Of the 4 EP subtypes, in situ hybridization and RT-PCR analysis showed that EP_2, EP_3, and EP_4 mRNAs were expressed in bile duct tissues (mostly the proliferating glandular elements, including mucus glands, and the lining epithelia with hyperplastic change) and biliary epithelial cells. It is of particular interest to determine the biological effect of PGE_2 on biliary epithelial cells via EP subtypes.

Because of the absence of a suitable human cholangiocyte cell line, a biliary adenocarcinoma cell line (Mz-ChA-2) was used for this study. The biological properties

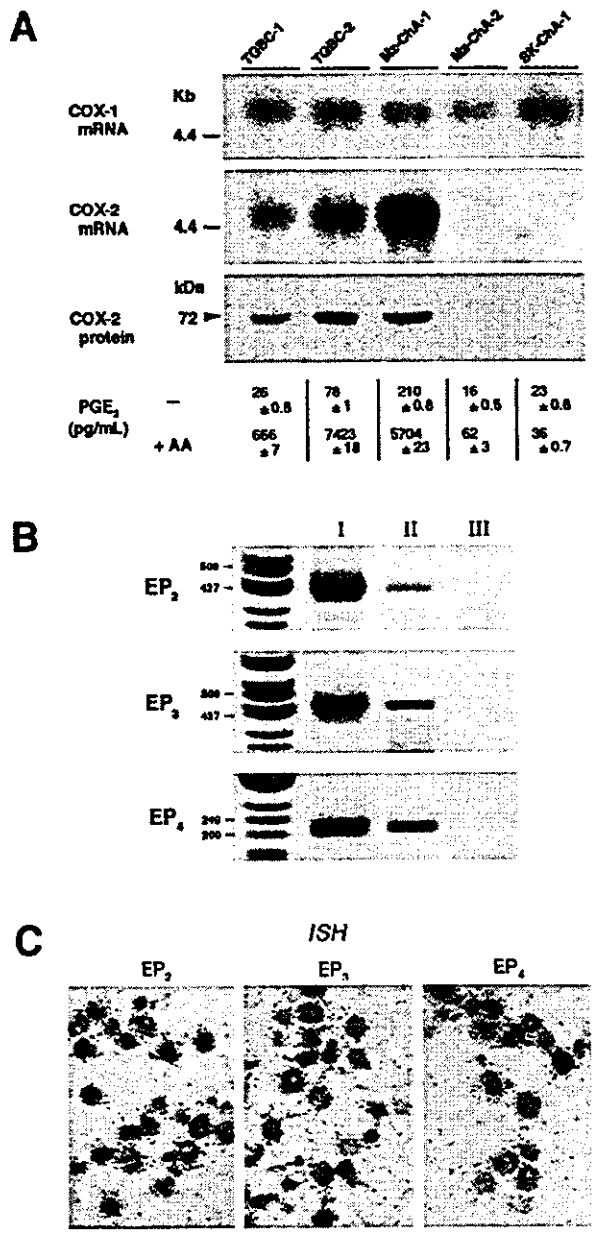

Figure 4. Characterization of biliary epithelial TGBC-1, TGBC-2, Mz-ChA-1, Mz-ChA-2, and Sk-ChA-1 cells. (*A*) Expression levels of COX-2 in the TGBC-1, TGBC-2, Mz-ChA-1, Mz-ChA-2, and Sk-ChA-1 cells. COX-2 protein and mRNA were expressed strongly in the TGBC-1, TGBC-2, and Mz-ChA-1 cells but were hardly detectable in the Mz-ChA-2 and Sk-ChA-1 cells. The former 3 cell lines were observed to produce significant amounts of PGE_2 in response to treatment with 50 μmol/L arachidonate, whereas the latter 2 cell lines were observed to produce only trace amounts. The results are expressed as means ± SEM, and the experiment was performed in triplicate. (*B*) RT-PCR and in situ hybridization of EP_{2-4} mRNAs in the Mz-ChA-2 cells. In the RT-PCR, the mRNAs of EP_2, EP_3, and EP_4 are amplified in the cells. *Lane I*, the PCR products from positive control cDNAs; *lane II*, the PCR products of expected size from the Mz-ChA-2 mRNA; *lane III*, RT-negative controls. (*C*) In the in situ hybridization, EP_2, EP_3, and EP_4 mRNAs in the Mz-ChA-2 cells. The mRNAs of EP_2, EP_3, and EP_4 were diffusely and strongly expressed in the cells.

Table 5. Effects of EP_{2-4}-Selective Agonists and an EP_4-Selective Antagonist on DNA Synthesis, Colony Formation, and Mucin Secretion in Mz-ChA-2 Cells

	μmol/L	DNA synthesis (% of nontreated cells)	Colony no.	Mucin secretion (% of nontreated cells)
No treatment	—	100 ± 8	211 ± 12	100 ± 5
PGE_2	1	221 ± 19[a]	390 ± 15[a]	176 ± 18[a]
ONO-AE1-259 (EP_2-selective agonist)	0.01	102 ± 9	227 ± 13	106 ± 11
	0.1	114 ± 12	232 ± 18	105 ± 6
	1	115 ± 11	237 ± 15	113 ± 10
	10	99 ± 8	222 ± 10	98 ± 9
ONO-AE-248 (EP_3-selective agonist)	0.01	109 ± 12	228 ± 17	96 ± 5
	0.1	102 ± 10	216 ± 14	95 ± 8
	1	95 ± 7	222 ± 11	97 ± 10
	10	89 ± 11	212 ± 15	89 ± 7
ONO-AE1-329 (EP_4-selective agonist)	0.01	123 ± 13	266 ± 13[a]	107 ± 6
	0.1	168 ± 18[a]	356 ± 16[a]	125 ± 10[b]
	1	193 ± 19[a]	407 ± 18[a]	155 ± 18[a]
	10	112 ± 14	283 ± 12[a]	104 ± 7
PGE_2 (1 μmol/L) + ONO-AE3-208 (EP_4-selective antagonist)	0.01	179 ± 18[a,c]	180 ± 16[c]	100 ± 8[c]
	0.1	136 ± 13[a,c]	161 ± 17[a,c]	85 ± 13[c]
	1	131 ± 15[a,c]	141 ± 12[a,c]	69 ± 10[b,c]
	10	133 ± 13[a,c]	143 ± 13[a,c]	75 ± 12[c]

NOTE. Values are given as means ± SEM of quadruplicate wells.
[a]$P < 0.01$, significantly different from nontreated cells.
[b]$P < 0.05$, significantly different from nontreated cells.
[c]$P < 0.01$, significantly different from PGE_2-treated cells.

of Mz-ChA-2 cells have been described by Knuth et al.[37] For the colony formation, Mz-ChA-2 cells show the adherent cell growth of typical epithelial cell types in cultures, and the cells regularly form gland-like structures in cell cultures. Importantly, the expression levels of EP subtypes in Mz-ChA-2 cells were quite similar to those in the bile ducts of patients with hepatolithiasis, whereas the expression levels in murine gallbladder and bile duct tissues (EP_1 and EP_2 subtypes predominate; unpublished observation, October, 2002) were significantly different from those in the bile ducts of patients with hepatolithiasis. In this regard, animal models may not be suitable to study the effects of EP_4 agonist or antagonist on experimental cholangitis (e.g., bile duct ligation).

Table 6. Production of Intracellular cAMP by Mz-ChA-2 Cells After Stimulation With EP-Receptor Agonists or Antagonist

	μmol/L	pmol intracellular cAMP/mg protein
No treatment	—	26.4 0.9
ONO-AE-259 (EP_2-selective agonist)	1	57.2 1.8[a]
ONO-AE-248	0.01	33.4 2.4
	0.1	35.3 0.8
	1	24.0 1.1
ONO-AE1-329 (EP_4-selective agonist)	0.01	47.0 2.2
	0.1	190.7 6.7[b]
	1	313.7 16.8[b]
ONO-AE3-208 (EP_4-selective agonist)	0.01	26.4 0.2
	0.1	24.9 0.4
	1	25.5 0.4
PGE_2	1	275.7 29.5[b]
PGE_2 (1 μmol/L) + ONO-AE3-208	0.01	191.4 8.7[c]
	0.1	47.1 1.8[c]
	1	32.3 0.6[c]

NOTE. Values are given as means ± SEM of triplicate experiments.
[a]$P < 0.05$, significantly different from nontreated cells.
[b]$P < 0.01$, significantly different from nontreated cells.
[c]$P < 0.01$, significantly different from PGE_2-treated cells.

In in vitro experiments, the effect of treatment with EP-selective agonists as well as PGE_2 on DNA synthesis and formation of colonies by plating biliary adenocarcinoma cells (Mz-ChA-2) in a monolayer culture was determined. An important finding is that treatment with an EP_4 agonist significantly increased DNA synthesis and colony number of Mz-ChA-2 cells in a dose-dependent manner. In addition, the treatment significantly increased the amount of mucin secretion in the cells in a dose-dependent manner. On the other hand, treatment with an EP_4 antagonist abolished the biological effects of PGE_2 on the cells. A key step by which PGE_2 potentiates proliferation or mucin secretion in the cells may be activation of EP_4, as was recently observed in colonic epithelial cells.[49,50]

Activation of EP_4 in Mz-ChA-2 cells was confirmed by the finding of significant increases in intracellular cAMP concentrations evoked by PGE_2 or the EP_4 agonist and by the finding of significant inhibition of the PGE_2-

evoked increases in intracellular cAMP concentrations by the EP_4 antagonist (Table 6). Regarding the stimulation of DNA synthesis in the cells in response to EP_4 activation, in the adenylate cyclase pathway, increased intracellular cAMP levels may result in activation of cAMP-dependent protein kinase (protein kinase A) and a transcriptional factor that binds to cAMP-responsive elements to transactivate the transcription of specific primary response genes that initiate cell proliferation.[51] The activation of EP_4 would mediate signals inside the nucleus to induce c-*fos* gene transcription, and the increased expression level of c-*fos*, a growth-related proto-oncogene, may at least in part account for the observed promotion of growth of the cells.[36] Furthermore, the stimulation of mucin secretion and cAMP production in the cells by the EP_4 agonist and the inhibition of PGE_2-stimulated mucin secretion and cAMP production in the cells by the EP_4 antagonist suggest that PGE_2 interacts at EP_4 to induce cAMP-dependent mucin exocytosis in the cells.

Hepatolithiasis has a high rate of recurrence. The overall recurrence rate was 6.6% in a recent survey in Japan.[52] This is in sharp contrast to ordinary cholelithiasis. Moreover, the results of recent surveys in Japan on postsurgical prognosis of 303 patients with hepatolithiasis over a 10-year period showed that 12% of the patients still had symptoms associated with cholangitis and 30% had died, mostly because of cholangiocarcinoma.[52] Thus, postsurgical morbidity is substantial. Therapeutic options for hepatolithiasis are still limited. Some adjuvant chemotherapies targeting pathobiological factors involved in cholangitis or chemopreventive therapies against inflammation-associated carcinogenesis in the biliary tract would be preferable for intractable cases. The results of the present study suggest that selective COX-2 inhibitors or EP_4-selective antagonists may be potent candidates as therapeutic agents for the disease.

In summary, the results of this study suggest that an enhanced synthesis of PGE_2 and its actions mediated via the EP_4 receptor in the bile ducts may be of pathobiological significance for chronic proliferative cholangitis in patients with hepatolithiasis.

References

1. Nakayama F, Koga A. Hepatolithiasis: present status. World J Surg 1984;8:9–14.
2. Nakayama F, Soloway RD, Nakama T, Miyazaki K, Ichimiya H, Sheen PC, Ker CG, Ong GB, Choi TK, Boey J, et al. Hepatolithiasis in East Asia. Retrospective study. Dig Dis Sci 1986;31:21–26.
3. Suzuki N, Takahashi W, Sato T. Types and chemical composition of intrahepatic stones. In: Okuda K, Nakayama F, Wong J, eds. Intrahepatic calculi. Progress in clinical and biological research. Volume 152. New York: Liss, 1984:71–80.
4. Trotman BW, Ostrow JD, Soloway RD. Pigment vs cholesterol cholelithiasis: comparison of stone and bile composition. Am J Dig Dis 1974;19:585–590.
5. Miyake H, Johnston CG. Etiological studies. Digestion 1968;1: 219–228.
6. Soloway RD, Trotman BW, Ostrow JD. Pigment gallstone. Gastroenterology 1977;72:167–182.
7. Maki T. Pathogenesis of calcium bilirubinate gallstone: role of *E. coli*, β-glucuronidase and coagulation by inorganic ions, polyelectrolytes and agitation. Ann Surg 1966;164:90–100.
8. Masuda H, Nakayama F. Composition of bile pigment in gallbladder stones and bile and their etiological significance. J Lab Clin Med 1979;93:353–360.
9. Ohta G, Nakanuma Y, Terada T. Pathology of hepatolithiasis: cholangitis and cholangiocarcinoma. In: Okuda K, Nakayama F, Wong J, eds. Intrahepatic calculi. Progress in clinical and biological research. Volume 152. New York: Liss, 1984:91–113.
10. Nakanuma Y, Yamaguchi K, Ohta G, Terada T. Japanese Hepatolithiasis Study Group. Pathologic features of hepatolithiasis in Japan. Hum Pathol 1988;19:1181–1186.
11. Ohta T, Nakagawa T, Yoshimitsu Y, Sanada H, Fonseca L, Miyazaki I, Terada T. The role of 16,16-dimethyl prostaglandin E_2 on the intrahepatic biliary branches in dogs. Hepatology 1993; 17:1062–1065.
12. Robert A, Nezamis JE, Phillips JP. Effect of prostaglandin E_1 on gastric secretion and ulcer formation in the rat. Gastroenterology 1979;55:481–487.
13. Eberhart CE, Dubois RN. Eicosanoids and the gastrointestinal tract. Gastroenterology 1995;109:285–301.
14. Blikslager AT, Roberts MC, Rhoads JM, Argenzio RA. Prostaglandin I_2 and E_2 have a synergistic role in rescuing epithelial barrier function in porcine ileum. J Clin Invest 1997;100:1928–1933.
15. Ding M, Kinoshita Y, Kishi K, Nakata H, Hassan S, Kawanami C, Sugimoto Y, Katsuyama M, Negishi M, Narumiya S, Ichikawa A, Chiba T. Distribution of prostaglandin E receptors in the rat gastrointestinal tract. Prostaglandins 1997;53:199–216.
16. Morimoto K, Sugimoto Y, Katsuyama M, Oida H, Tsuboi K, Kishi K, Kinoshita Y, Negishi M, Chiba T, Narumiya S, Ichikawa A. Cellular localization of mRNAs for prostaglandin E receptor subtypes in mouse gastrointestinal tract. Am J Physiol 1997;272: G681–G687.
17. Shoda J, Ueda T, Ikegami T, Matsuzaki Y, Satoh S, Kano M, Matsuura K, Tanaka N. Increased biliary group II phospholipase A_2 and altered gallbladder bile in patients with multiple cholesterol stones. Gastroenterology 1997;112:2036–2047.
18. Shoda J, Kano M, Asano T, Irimura T, Ueda T, Iwasaki R, Furukawa M, Kamiya J, Nimura Y, Todoroki T, Matsuzaki Y, Tanaka N. Secretory low-molecular-weight phospholipases A_2 and their specific receptor in bile ducts of patients with intrahepatic calculi: factors of chronic proliferative cholangitis. Hepatology 1999;29: 1026–1036.
19. Nakayama F. Intrahepatic calculi: a special problem in East Asia. World J Surg 1982;6:802–804.
20. Trotman BW, Soloway RD. Pigment gallstone disease: summary of the National Institutes of Health—International Workshop. Hepatology 1982;2:879–884.
21. Trotman BW, Morris TA, Sanchez HM, Soloway RD, Ostrow JD. Pigment versus cholesterol cholelithiasis: identification and quantitation by infrared spectroscopy. Gastroenterology 1977; 72:495–498.
22. Nishijima J, Okamoto M, Ogawa M, Kosaki G, Yamano T. Purification and characterization of human pancreatic phospholipase A_2 and development of a radioimmunoassay. J Biochem 1983; 94:137–147.
23. Tojo H, Ono T, Okamoto M. Reverse-phase high performance liquid chromatographic assay of phospholipases: application of spectrophotometric detection to rat phospholipase A_2 isozymes. J Lipid Res 1993;34:837–844.

24. Broomfield PH, Chopra R, Sheinbaum RC, Bonorris GG, Silverman A, Schoenfield LE, Marks JW. Effects of ursodeoxycholic acid and aspirin on the formation of lithogenic bile and gallstones during loss of weight. N Engl J Med 1988;319:1567–1572.
25. Miquel JF, Grõen AK, van Wijland MJA, Del Pozo R, Eder MI, von Ritter C. Quantitation of mucin in human gallbladder bile: a fast, specific and reproducible method. J Lipid Res 1995;36:2450–2458.
26. Crowther RS, Wetmore RF. Fluorometric assay of O-linked glycoproteins by reaction with 2-cyanoacetamide. Anal Biochem 1987; 163:170–174.
27. Kawamoto T, Shoda J, Asano T, Ueda T, Furukawa M, Koike N, Fukao K, Tanaka N, Todoroki T. Expression of cyclooxygenase-2 in the subserosal layer correlates with postsurgical prognosis of pathological tumor stage 2 carcinoma of the gallbladder. Int J Cancer 2002;98:427–434.
28. Chomczynski P, Sacchi N. Single step method for RNA isolation by acid guanidinium thioctanaic-phenol-chloroform extraction. Anal Biochem 1987;162:156–159.
29. Yokoyama C, Tanabe T. Cloning of human gene encoding prostaglandin endoperoxide synthetase and primary structure of the enzyme. Biochem Biophys Res Commun 1989;165:888–894.
30. Kasaka T, Miyata A, Ihara H, Hara S, Sugimoto T, Takeda O, Takahashi E, Tanabe T. Characterization of the human gene (PTGS2) encoding prostaglandin-endoperoxide synthetase 2. Eur J Biochem 1994;221:889–897.
31. Kramer RM, Hession C, Johansen B, Hayes G, McGray P, Chow EP, Tizard R, Pepinsky RB. Structure and properties of a human non-pancreatic phospholipase A_2. J Biol Chem 1989;264:5768–5775.
32. Funk CD, Furci GA, Grygorczyk R, Rochette C, Bayne MA, Abramovitz M, Adam M, Metters KM. Cloning and expression of a cDNA for the human prostaglandin E receptor EP_1 subtype. J Biol Chem 1993;268:26767–26772.
33. Regan JW, Bailey TJ, Pepperl DJ, Pierce KL, Bogardus AM, Donello JE, Fairbraim CE, Kedzie KM, Woodward DF. Cloning of a novel human prostaglandin receptor with characteristics of the pharmacologically defined EP_2 subtype. Mol Pharmacol 1994;48: 213–220.
34. Schmid A, Thierauch K-H, Schleuning W-D, Dinter H. Splice variants of the human EP_3 receptor for prostaglandin E_2. Eur J Biochem 1995;228:23–30.
35. Bastien L, Sawyer N, Grygorczyk R, Metters KM, Adam M. Cloning, functional expression, and characterization of the human prostaglandin E_2 receptor EP_2 subtype. J Biol Chem 1994;269: 11873–11877.
36. Asano T, Shoda J, Ueda T, Kawamoto T, Todoroki T, Shimonishi N, Tanabe T, Sugimoto Y, Ichikawa A, Mutoh M, Tanaka N, Miwa M. Expression of cyclooxygenase-2 and prostaglandin E-receptors in carcinoma of the gallbladder: crucial role of arachidonate metabolism in tumor growth and progression. Clin Cancer Res 2002;8:1157–1167.
37. Knuth A, Gabbert H, Dippold W, Klein O, Sachsse W, Bitter-Suermann D, Prellwitz W, Meyer zum Büschenfelde KH. Biliary adenocarcinoma characterization of three new human tumor cell lines. J Hepatol 1985;1:579–596.
38. Koike N, Todoroki T, Kawamoto T, Yoshida S, Kashiwagi H, Fukao K, Ohno T, Watanabe T. The invasion potentials of human biliary tract carcinoma cell lines: correlation between invasiveness and morphologic characteristics. Int J Oncol 1998;13:1269–1274.
39. Suzawa T, Miyaura C, Inada M, Maruyama T, Sugimoto Y, Ushikubo F, Ichikawa A, Narumiya S, Suda T. The role of prostaglandin E receptor subtypes (EP_1, EP_2, EP_3, and EP_4) in bone resorption: an analysis using specific agonists for the respective EPs. Endocrinology 2000;141:1554–1559.
40. Kabashima K, Saji T, Murata T, Nagamachi M, Matsuoka T, Segi E, Tsuboi K, Sugimoto Y, Kobayashi T, Miyaxhi Y, Ichikawa A, Narumiya S. The prostaglandin receptor EP_4 suppresses colitis, mucosal damage and CD4 cell activation in the gut. J Clin Invest 2002;109:883–893.
41. Sheng H, Shao J, Morrow JD, Beauchamp RD, Dubois RN. Modulation of apoptosis and bcl-2 expression by prostaglandin E_2 in human colon cancer cells. Cancer Res 1998;58:362–366.
42. Klinkspoor JH, Kuber R, Savard CE, Oda D, Azzouz H, Tytgat GNJ, Grõen AK, Lee SP. Model bile and bile salts accelerate mucin secretion by cultured dog gallbladder epithelial cells. Gastroenterology 1995;109:264–274.
43. Shoda J, He B, Tanaka N, Matsuzaki Y, Shyunji Y, Osuga T. Primary dual defect of cholesterol and bile acid metabolism in liver of patients with intrahepatic calculi. Gastroenterology 1995; 108:1534–1546.
44. Shoda J, Oda K, Suzuki H, Sugiyama Y, Ito K, Cohen DE, Feng L, Kamiya J, Nimura Y, Miyazaki H, Kano M, Matsuzaki Y, Tanaka N. Etiological significance of metabolic defects of cholesterol, phospholipid, and bile acid in the liver of patients with intrahepatic calculi. Hepatology 2001;33:1194–1205.
45. Sheng H, Shao J, Morrow JD, Beauchamp RD, Dubois RN. Modulation of apoptosis and bcl-2 expression by prostaglandin E_2 in human colon cancer cells. Cancer Res 1998;58:362–366.
46. Hla T, Ristimaki A, Appleby S, Barriocanal JG. Cyclooxygenase gene expression in inflammation and angiogenesis. Ann N Y Acad Sci 1993;686:197–204.
47. Arita H, Hanasaki K, Nakano T, Oka S, Teraoka H, Matsumoto K. Novel proliferative effect of phospholipase A_2 in Swiss 3T3 cells via specific binding site. J Biol Chem 1991;266:19139–19141.
48. Eberhart CE, Dubois RN. Eicosanoids and the gastrointestinal tract. Gastroenterology 1995;109:285–301.
49. Belley A, Chadee K. Prostaglandin E_2 stimulates rat and human colonic mucin exocytosis via the EP_4 receptor. Gastroenterology 1999;117:1352–1362.
50. Sheng H, Shao J. Washington MK, DuBois RN. Prostaglandin E_2 increases growth and motility of colorectal carcinoma cells. J Biol Chem 2001;276:18075–18081.
51. Dhanasekaran N, Tsim ST, Dermott JM, Onesime D. Regulation of cell proliferation by G proteins. Oncogene 1998;17:1383–1394.
52. Tanimura H, Uchiyama K, Ishimoto K, Nagai K. Epidemiology of hepatolithiasis in Japan (in Japanese). Annual reports of the Japanese Ministry of Health and Welfare. Tokyo, Japan: 1994:17–27.

Address requests for reprints to: Junichi Shoda, M.D., Ph.D., Department of Gastroenterology, Institute of Clinical Medicine, University of Tsukuba, 1-1-1 Tennodai, Tsukuba-shi, Ibaraki 305-8575, Japan. e-mail: shodaj@md.tsukuba.ac.jp; fax: (81) 298-53-3124.

Supported in part by grants-in-aid for hepatolithiasis from the Ministry of Health and Welfare, Japan, and grants-in-aid from the University of Tsukuba Research Projects, Japan.

Available online at www.sciencedirect.com
SCIENCE DIRECT®
Pergamon
Neuropharmacology 45 (2003) 96–105
NEURO PHARMACOLOGY
www.elsevier.com/locate/neuropharm

Functional evidence for interaction between prostaglandin EP3 and κ-opioid receptor pathways in tactile pain induced by human immunodeficiency virus type-1 (HIV-1) glycoprotein gp120

Toshiaki Minami [a], Shinji Matsumura [b], Tamaki Mabuchi [b], Takuya Kobayashi [c], Yukihiko Sugimoto [d], Fumitaka Ushikubi [e], Atsushi Ichikawa [d], Shuh Narumiya [c], Seiji Ito [b,*]

[a] *Department of Anesthesiology, Osaka Medical College, Takatsuki 569-8686, Japan*
[b] *Department of Medical Chemistry, Kansai Medical University, Moriguchi 570-8506, Japan*
[c] *Department of Pharmacology, Faculty of Medicine, Kyoto University, Kyoto 606-8315, Japan*
[d] *Department of Physiological Chemistry, Faculty of Pharmaceutical Sciences, Kyoto University, Kyoto 606-8315, Japan*
[e] *Department of Pharmacology, Asahikawa Medical College, Asahikawa 078-8510, Japan*

Received 9 August 2002; received in revised form 10 February 2003; accepted 13 March 2003

Abstract

HIV-1 glycoprotein gp120 administered intrathecally induces tactile pain (allodynia) in animals. In the present study, we investigated the mechanism of gp120-induced allodynia and possible functional connections with factors modulating pain transmission at the spinal level. Gp120 evoked allodynia in a dose-dependent manner with the maximum effect at 1 pg/mouse, and stimulated a rapid increase in intracellular free Ca^{2+} concentration ($[Ca^{2+}]i$) in the dorsal horn cells of the spinal cord. These responses evoked by gp120 were blocked by galactocerebroside. The gp120-induced allodynia was also attenuated by the non-steroidal anti-inflammatory drug indomethacin, which inhibits prostaglandin synthesis, and did not develop in mice lacking the EP3 prostaglandin E receptor subtype ($EP3^{-/-}$). Pretreatment of spinal slices with indomethacin dose-dependently decreased the percentage of the cells that showed increased $[Ca^{2+}]i$ in response to gp120, and the decrease was reversed by addition of the selective EP3 agonist ONO-AE-248. The κ-opioid agonist U-50,488 significantly enhanced the gp120-stimulated increase in $[Ca^{2+}]i$ in spinal slices prepared from $EP3^{-/-}$ mice, and the simultaneous addition of U-50,488 with gp120 reproduced the gp120-induced allodynia in $EP3^{-/-}$ mice. These results suggest that gp120 induced allodynia by increasing $[Ca^{2+}]i$, concomitant with activation of prostanoid EP3 and κ-opioid receptors in the spinal cord.

Keywords: Allodynia (tactile pain); Intrathecal; Knockout mice; κ-Opioid receptor; Prostanoid EP3 receptor

1. Introduction

The human immunodeficiency virus type-1 (HIV-1) is highly neurotropic and invades nervous system structures early in the course of HIV-1 infection (Epstein and Gendelman, 1993). A portion of patients with acquired immune deficiency syndrome (AIDS) suffer from neurological diseases such as AIDS dementia complex characterized by cognitive and motor deficits (Epstein and Gendelman, 1993) and a symmetrical predominantly sensory neuropathy often associated with painful symptoms (Cornblath and McArthur, 1988; O'Neill and Sherrard, 1993; Breitbart, 1997). Recent in vivo and in vitro studies suggested both direct and indirect roles for HIV-1 glycoprotein gp120 in the neurological complications associated with AIDS.Gp120 produced in the brain and spinal cord of transgenic mice induced a spectrum of neuronal and glial changes resembling abnormalities seen in the nervous system of HIV-1-infected humans (Thomas et al., 1994; Toggas et al., 1994). Exposure of several types of neuronal cells in culture to gp120 led

* Corresponding author. Tel.: +81-6-6993-9425; fax: +81-6-6992-1781.
E-mail address: ito@takii.kmu.ac.jp (S. Ito).

0028-3908/03/$ - see front matter © 2003 Elsevier Science Ltd. All rights reserved.
doi:10.1016/S0028-3908(03)00133-3

to cell death along a pathway that might involve the activities of phospholipase A_2 (Ushijima et al., 1995) and cyclooxygenase (COX), enzymes responsible for prostaglandin (PG) production (Epstein and Gendelman, 1993; Maccarrone et al., 1998; Corasaniti et al., 2000). PGs are a group of bioactive lipids produced from arachidonic acid, and PGE_2 is the major in vivo product of COX under pathophysiological conditions (Vane et al., 1998; Narumiya et al., 1999). Indeed, gp120 enhanced PGE_2 production in the rat neocortex; and the non-steroidal anti-inflammatory drug (NSAID) indomethacin or NS398, which exerts its action by inhibiting COX, protected the cells against gp120-induced cell death (Bagetta et al., 1998; Corasaniti et al., 2000; Maccarrone et al., 2000). Thus disturbances in the arachidonate cascade have been proposed to play a role in HIV-1 pathogenesis.

Painful peripheral neuropathies due to HIV-1 infection are characterized by hyperalgesia and allodynia (brush-evoked pain; Bouhassira et al., 1999). Recently, it was shown that the intrathecal (*i.t.*) injection of gp120 into rats induced thermal hyperalgesia and allodynia (Watkins and Maier, 1999; Milligan et al., 2000). Although the mechanisms through which peripheral neuropathies develop in AIDS are still unclear, allodynia is viewed as neural phenomenon that reflects changes in neuronal excitability in the spinal dorsal horn (Woolf, 1994; Yaksh et al., 1999). We previously showed that the *i.t.* injection of PGE_2 or $PGF_{2\alpha}$ induced allodynia in conscious mice (Minami et al., 1994, 1999). PGs produce a broad range of biological effects by interacting with their respective receptors on plasma membranes, and the diversity of PGE_2 actions is considered to be the result of PGE receptor subtypes EP1 to EP4 (Narumiya et al., 1999). Knockout mice lacking respective PGE receptor subtypes have enabled us to assign actions of PGE_2 such as pain and fever to a given PGE receptor subtype (Ushikubi et al., 1998; Minami et al., 2001; Ueno et al., 2001). In the present study, we investigated the possible role of PGs in gp120-induced allodynia by use of indomethacin and EP1 and EP3 knockout ($EP1^{-/-}$ and $EP3^{-/-}$) mice. Furthermore, we examined the functional connection with factors modulating pain transmission at the spinal level.

2. Materials and methods

2.1. Intrathecal injection and allodynia

Male ddY mice and C57BL/6 mice were obtained from a local distributor. $EP1^{-/-}$ and $EP3^{-/-}$ mice were generated as described previously (Ushikubi et al., 1998), and back-crossed over at least six generations to C57BL/6 mice. The animals were housed under conditions of a 12-h light/12-h dark cycle, a constant temperature of 22 ± 2 °C, and 60 ± 10% humidity. They were allowed free access to food and water before testing. All chemicals were dissolved in sterile saline on the day of the experiments and kept on ice until used. All drugs including saline were coded to assure blind testing. A 27-gauge stainless-steel needle (0.35 mm, o.d.) attached to a microsyringe was inserted between the L5 and L6 vertebrae, and 5 μl of drug solution or physiological saline was injected slowly into the subarachnoid space of conscious mice.

Four-week-old ddY male mice weighing 20 ± 2 g, and weight-matched $EP1^{-/-}$ and $EP3^{-/-}$ mice were used for assessing allodynia. Allodynia was analyzed as described previously (Minami et al., 1999). Briefly, allodynia was measured every 5 min over a 50-min period by light stroking of the flank of the mice with a paintbrush. The allodynic response was ranked as 0–2 as follows: 0, no response; 1, mild squeaking with attempts to move away from the stroking probe; 2, vigorous squeaking evoked by the probe, biting at the probe or strong efforts to escape. For the time course of allodynia, data ($n = 6$) were expressed as a percent of the maximum possible cumulative score evaluated every 5 min. Thus the maximum possible cumulative score for allodynia in any 5-min period was 12 (2×6) and was taken 100%. For the evaluation of the effect of drugs on gp120-induced allodynia, data ($n = 6$) were expressed as a percent of the maximum possible cumulative score over the 50-min experiment period. Thus the maximum possible cumulative score of allodynia for 50 min was 120 ($2 \times 6 \times 10$) and was taken as 100%. The animals were used only for one experiment.

This study was conducted with the approval of the animal experimentation committees of Kansai Medical University and Osaka Medical College, and in accordance with the guidelines of the Ethics Committee of the International Association for the Study of Pain (Zimmermann, 1983).

2.2. Slice preparation

Slices were prepared from the lumbar spinal cord of 2-week-old C57BL/6 and $EP3^{-/-}$ mice. After the animal had been anesthetized with ethyl ether, the spinal cord was dissected by quickly cutting the vertebral arcs at the lateral side of thoracic to sacral regions. The spinal cord was immediately placed in artificial cerebrospinal fluid (ACSF) equilibrated with 95% O_2/5% CO_2 and maintained in ice-cold ACSF. Roots and meninges were removed, and lumbosacral segments L3-S2 of the spinal cord were embedded in ACSF containing 3% low-melting agar. Lumbosacral segments were cut by using a vibrating blade microtome (Leica VT-1000S, Nussloch, Germany), and slices (300-μm thick) obtained from lumbar segments L4–L6 were used for calcium measurement.

ACSF of the following composition was used (in mM): 120 NaCl, 3.1 KCl, 2.0 $CaCl_2$, 1.0 $MgCl_2$, 1.25 NaH_2O_4, 25 $NaHCO_3$, 5.0 glucose, 2.0 sodium pyruvate, 0.5 *myo*-inositol, and 0.02 ascorbic acid.

2.3. Calcium measurement

After 3-h incubation of the slices in ACSF bubbled with 95% O_2/5% CO_2 at 37 °C, slices were loaded with fura-2 by incubating them for 2 h at room temperature in Krebs' solution containing 10 μM fura-2-acetoxymethyl ester (Dojindo Chemical, Kumamoto, Japan) and 0.01% cremophor EL (Sigma-Aldrich, St. Louis, MO). The slices were kept in Krebs' solution for more than 1 h after loading, and then they were placed in the recording chamber that was mounted on an inverted fluorescence microscope (IX-70, Olympus, Tokyo, Japan) and mechanically fixed in place by using an overlaying grid of nylon threads attached to a platinum ring. The slice was superfused in Krebs' solution equilibrated with 95% O_2/5% CO_2 at 3 ml/min. The intracellular free Ca^{2+} concentration ($[Ca^{2+}]i$) was measured as a fluorescence ratio obtained with excitation at 340 and 380 nm. Optical signals were recorded by using an Argus-HiSCA imaging system (Hamamatsu Photonics, Shizuoka, Japan) equipped with a cooled charge-coupled device camera.

2.4. Drugs

11,15-*O*-dimethyl PGE_2 (ONO-AE-248), a selective EP3 agonist (Zacharowski et al., 1999), was a generous gift from Ono Central Research Institute (Osaka, Japan). Morphine was purchased from Takeda Chemical Industry (Osaka, Japan). [D-Ala^2, *N*-methyl-Phe^4, Gly^5-ol]-enkephalin (DAMGO, a μ-opioid receptor agonist), [D-Pen^{2,5}]-enkephalin (DPDPE, a δ-opioid receptor agonist), *trans*-(±)-3,4-dichloro-*N*-methyl-*N*-(2-[1-pyrrolidinyl] cyclohexyl) benzeneacetamide (U-50,488, a κ-opioid receptor agonist), and nor-binaltorphimine (nor-BNI, a κ-opioid receptor antagonist) were obtained from Sigma-Aldrich. HIV-1_{IIIB} gp120 and horseradish peroxidase (HRP)-gp120 were supplied by Diagnostics (Buffalo, NY). All other chemicals were of analytical grade and purchased from Wako Pure Chemicals (Osaka, Japan).

2.5. Statistics

Data for allodynia were analyzed by non-parametric analyses of variance. Statistical significance ($P < 0.05$) was further examined by using the Mann-Whitney *U* test for multiple comparison. ID_{50} values with 95% confidence limits (95% CL) were calculated by use of the computer program FIG-P (Biosoft, U.K.). Data for $[Ca^{2+}]i$ were analyzed by using a contingency table, and the Chi-square test was used as a post hoc test. $P < 0.05$ was considered significant.

3. Results

3.1. Involvement of prostaglandin (PG) in mechanical allodynia induced by gp120

Intrathecal injection of gp120 resulted in prominent allodynic responses, such as vocalization, biting, and escape from the probe, to tactile stimuli applied to the flank of conscious ddY mice. Fig. 1A presents time courses of brush-evoked allodynia induced by gp120 injected at 1 pg/mouse. The gp120-induced allodynia was evoked 5 min after *i.t.* injection, and intense brush-evoked allodynic responses were observed over a 50-min period. The response to gp120 at 1 pg was long lasting and did not disappear by 180 min (data not shown).When the scores of allodynia obtained for the overall 50 min were cumulated and expressed as a percent of the maximum possible score, gp120 increased the score in a dose-dependent manner. The allodynia was observed at a dose of as low as 0.01 fg of gp120/mouse, and the maximum effect (85 ± 7.5% of the 50-min maximum possible cumulative score) was observed at 1 pg/mouse (Fig. 1B). Whereas simultaneous *i.t.* injection of morphine showed no effect on the gp120-induced allodynia at doses up to 500 ng/mouse (Fig. 1A and D), the 60-min pretreatment of mice with orally administered indomethacin, a non-steroidal anti-inflammatory drug (NSAID), blocked the gp120-induced allodynia in a dose-dependent manner with an IC_{50} value (95% CL) of 43.3 ± 7.2 μg (± 15.0 μg) and almost completely abolished it at 0.1 mg/mouse (Fig. 1A and C).

NSAIIDs are known to exert their action by inhibiting PG production. To study the involvement of PGs in the gp120-induced allodynia and to assign it to a prostanoid receptor EP subtype, we examined the induction of allodynia in $EP1^{-/-}$ and $EP3^{-/-}$ mice. Intrathecal administration of gp120 (1 pg/mouse) caused prominent allodynia in $EP1^{-/-}$ mice and wild-type ($EP^{+/+}$ and $EP3^{+/+}$) mice cognate to $EP1^{-/-}$ and $EP3^{-/-}$ mice (Fig. 2), as observed in ddY mice (Fig. 1A) and C57BL/6 mice (data not shown). On the other hand, the gp120-induced allodynia was not observed in the $EP3^{-/-}$ mice (Fig. 2B).

3.2. Action site of gp120 for induction of allodynia

To elucidate action sites of gp120, we used HRP-gp120, an adduct of gp120 with HRP, instead of gp120 for direct detection of binding sites in the lumbar spinal cord without the use of second antibodies. Fig. 3 shows a representative section from the upper lumbosacral enlargement (L4) stained with diaminobenzidine as chromogen. Rather large cells in the deeper dorsal horn were stained (Fig. 3A and B). Motor neurons in the ventral horn were also intensely stained for gp120, but cells in the white matter were not stained. HRP-gp120 binding

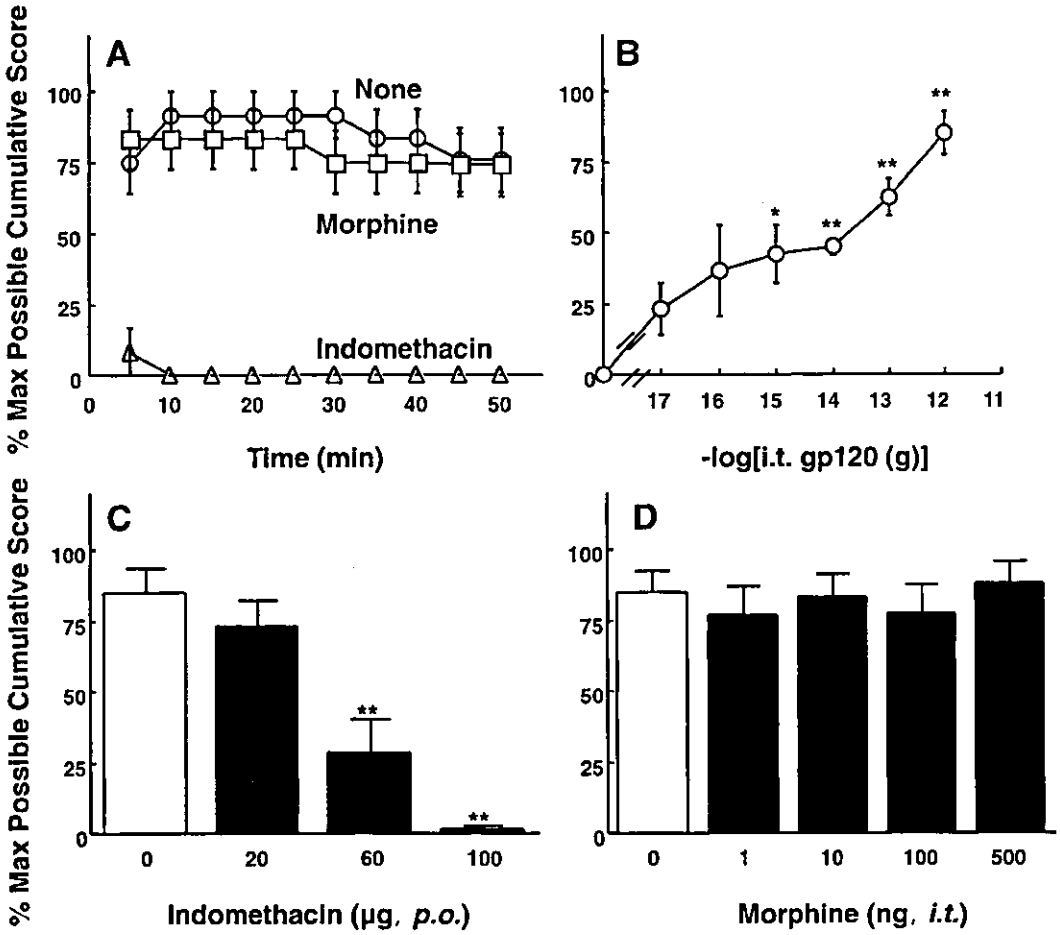

Fig. 1. Mechanical allodynia induced by gp 120 in ddY mice. (A) Time course of allodynia. Gp120 (1 pg/mouse) was injected into the subarachnoid space of conscious mice without (○) or with 100 ng of morphine (□) or with 60-min pretreatment with indomethacin (0.1 mg/mouse, *p.o.*) (△). Studies on allodynia were carried out as described under "Materials and methods". Each column (mean ± SEM) represents the percent of the maximum possible cumulative score of six mice evaluated every 5 min. Thus the maximum possible cumulative score for allodynia in any 5-min period was 12 (2 × 6) and was taken as 100%. (B) Dose dependency of allodynia. Various doses of gp120 were injected into the subarachnoid space of conscious mice. Data (mean ± SEM, $n = 6$) are expressed as a percent of the maximum possible cumulative score over the 50-min experiment period. Thus the maximum possible cumulative score of allodynia for 50 min was 120 (2 × 6 × 10) and was taken as 100%. $^{*}P < 0.05$; $^{**}P < 0.01$, as compared with the saline-injected group (Mann-Whitney *U* test). (C) Effect of oral indomethacin on gp120-induced allodynia. Indicated doses of indomethacin were orally administered 60 min before the *i.t.* injection of gp120 (1 pg/mouse). Data (mean ± SEM, $n = 6$) are expressed as a percent of the maximum possible cumulative score over the 50-min experiment period. $^{**}P < 0.01$, as compared with the gp120-injected group without indomethacin (Mann-Whitney *U* test). (D) Effect of *i.t.* morphine on gp120-induced allodynia. Indicated doses of morphine were *i.t.* injected simultaneously with gp120 (1 pg/mouse).

to the cells in the dorsal horn was blocked in the presence of galactocerebroside (Fig. 3C).

As shown in Fig. 4A, *i.t.* HRP-gp120 could induce allodynia in conscious mice with a time course similar to that induced by *i.t.* gp120 (Fig. IA). The allodynia induced by HRP-gp120 was completely blocked by the simultaneous injection of galactocerebroside in a dose-dependent manner, with an IC_{50} (95% CL) of 0.38 ± 0.17 μg (± 0.35 μg; Fig. 4B). These results suggest that gp120 and HRP-gp120 induced allodynia through binding to galactocerebroside on the cells. Because gp120 and HRP-gp 120 showed a comparable potency in induction of allodynia (Fig. 1A and 4A), HRP-gp120 was used in the subsequent in vitro experiments.

3.3. Increase in $[Ca^{2+}]i$ in spinal slices elicited by gp120

To study the action mechanism of gp120, we examined the $[Ca^{2+}]i$ response to gp120 in situ by using a total of 60 spinal slices from lumbar segments L4–L6 of 24 C57BL/6 mice. Fig. 5A illustrates a fura-2-loaded lumbar slice preparation under low magnification and a representative time course of the $[Ca^{2+}]i$ increase induced by HRP-gp120. HRP-gp120 could produce a rapid and transient increase in $[Ca^{2+}]i$. This $[Ca^{2+}]i$ increase was more obvious in the cells in the deeper laminae than in those in the superficial laminae of the spinal cord. While 57.1% of fura-2-loaded cells (535 out of 1107 cells in

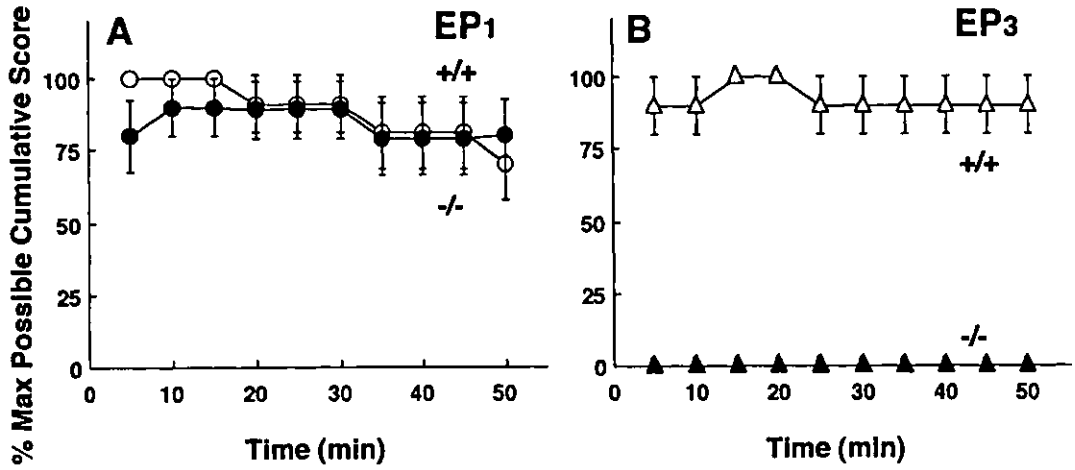

Fig. 2. Time courses of allodynia induced by gp120 in wild-type and EP receptor-deficient mice.(A) Gp120 (1 pg/mouse) was injected *i.t.* into the subarachnoid space of $EP1^{+/+}$ (○) and $EP1^{-/-}$ (●) mice.(B) Gp120 (1 pg/mouse) was injected *i.t.* into $EP3^{+/+}$ (△) and $EP3^{-/-}$ (▲) mice. Assessment of allodynia was made as described in the legend for Fig. 1A. The value (mean ± SEM) represents the percent of the maximum possible cumulative score of 5–6 mice evaluated every 5 min.

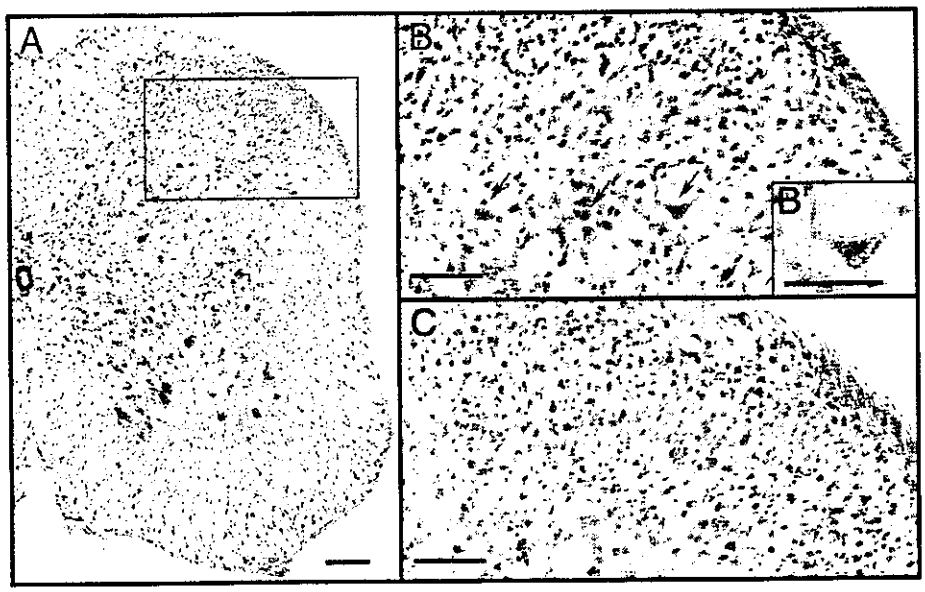

Fig. 3. Localization of gp120 binding in lumbar spinal cord.(A, B) Rather large cells in the deeper laminae of the dorsal horn and motor neurons were positively stained. "B" depicts a higher magnification of the dorsal horn of the spinal cord delineated by the rectangle in "A.". The arrow in "B" indicates a gp120-positive cell, which is magnified in the inset (B').(C) Galactocerebroside (100 μg/ml) blocked gp120 binding to the cells in the dorsal horn. After having been stained for gp120, the sections were lightly counterstained with hematoxylin. Scale bars (A–C) = 100 μm, scale bar (B') = 25 μm.

31 slices) in the laminae I-II increased $[Ca^{2+}]i$ by 2 nM HRP-gp120, more than 90% of the loaded cells (880 out of 969 cells in 29 slices) in the laminae III-VI responded to HRP-gp120. These gp120-responsive cells also showed an increase in $[Ca^{2+}]i$ by subsequent application of glutamate or *N*-methyl-D-aspartate. As shown in Fig. 5B, the $[Ca^{2+}]i$ increase elicited by HRP-gp120 in the deeper layer was abolished by coadministration of the glycoprotein and galactocerebroside.

3.4. Reproduction of gp120-induced allodynia in $EP3^{-/-}$ mice by κ-opioid agonist

To further study the role of the EP3 subtype in gp 120-induced allodynia, we sought an agent that could reproduce the allodynia in $EP3^{-/-}$ mice. As shown in Fig. 6, simultaneous injection of 5 pg of U-50,488, a κ-opioid agonist, with 1 pg of gp120 induced allodynia in the $EP3^{-/-}$ mice. Neither the μ-opioid agonist DAMGO nor

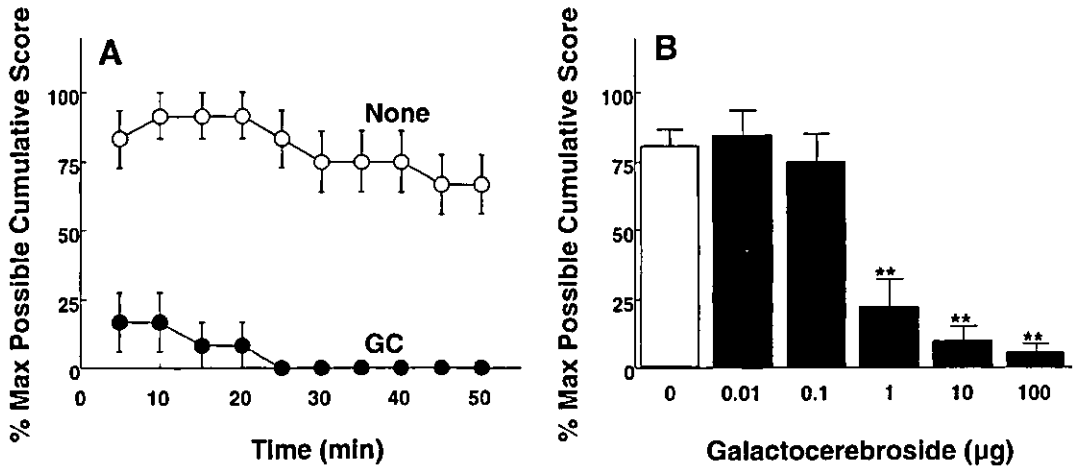

Fig. 4. Effect of galactocerebroside on gp120-induced allodynia. (A) Time course. HRP-gp120 (1 pg/mouse) was injected *i.t.* into conscious ddY mice without (○) or with (●) galactocerebroside (GC, 100 μg). Studies on allodynia were carried out as described in the legend for Fig. 1A.(B) Dose dependency. Indicated doses of galactocerebroside were *i.t.* injected simultaneously with gp120 (1 pg/mouse). Data (mean ± SEM, $n = 6$) are expressed as a percent of the maximum possible cumulative score over the 50-min experiment period. ** $P < 0.01$, as compared with the gp120-injected group without galactocerebroside (Mann-Whitney U test).

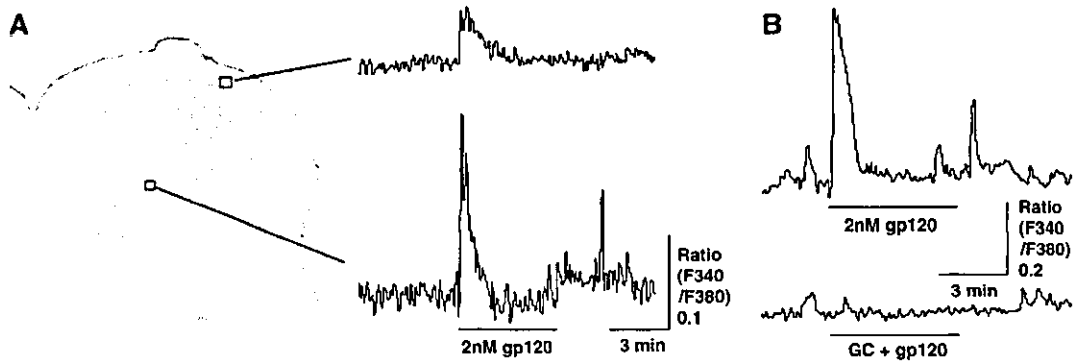

Fig. 5. $[Ca^{2+}]i$ changes by gp120 in the spinal cord.(A) Fluorescence image of fura-2-loaded slice from the lumbar spinal cord excited at 380 nm and $[Ca^{2+}]i$ changes elicited by gp120. $[Ca^{2+}]i$ was measured as a fluorescence ratio obtained with excitation at 340 and 380 nm as described under "Materials and methods".(B) Effect of galactocerebroside on $[Ca^{2+}]i$ change evoked by gp120. This image was obtained by applying 2 nM HRP-gp120 to a spinal slice followed by a second application of 2 nM HRP-gp120 + 200 μg galactocerebroside (GC) 25 min after the first application.

the δ-opioid agonist DPDPE at 5 pg was effective in reproducing gp120-induced allodynia in the $EP3^{-/-}$ mice. These results suggest that the EP3 subtype is involved in the gp120-induced allodynia, with its action possibly mediated by the κ-opioid pathway.

3.5. Action mechanism of induction of allodynia by gp120

To clarify the involvement of EP3 in the gp120-induced allodynia, we treated spinal slices prepared from C57BL/6 mice with indomethacin 3 h before the addition of 2 nM HRP-gp120. Pretreatment with indomethacin decreased the percentage of cells responsive to HRP-gp120 in a dose-dependent manner from 90.8 to 19.7% (Table 1). Conversely, the addition of the selective EP3 agonist ONO-AE-248 (10 μM) increased the percentage of gp120-responsive cells as the concentration of indomethacin was increased. Fig. 7A shows a representative time course of the $[Ca^{2+}]i$ increase in such cells. Pretreatment of spinal slices with indomethacin did not affect the increase in $[Ca^{2+}]i$ caused by glutamate or *N*-methyl-D-aspartate.

To further study the mechanism of reproduction of gp120-induced allodynia by U-50,488 in $EP3^{-/-}$ mice, we examined the effects of various agents on $[Ca^{2+}]i$ in the deeper laminae of spinal cord. In the first series of experiments, we assessed the effect of ONO-AE-248 on $[Ca^{2+}]i$ in spinal slices prepared from lumbar segments L4–L6 of $EP3^{-/-}$ mice. HRP-gp120 (2 nM) increased $[Ca^{2+}]i$ in a smaller percentage (31.9%) of cells (61 out of 191 cells), as compared with that percentage found for C57BL/6 mice. ONO-AE-248 (10 μM) neither increased $[Ca^{2+}]i$ in the cells that did not respond to HRP-gp120

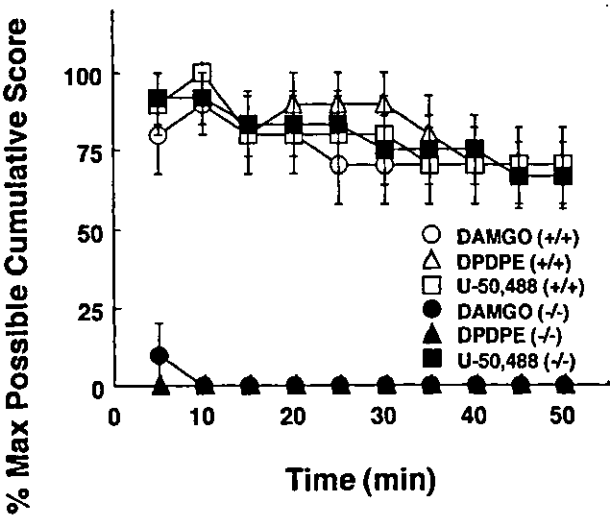

Fig. 6. Reproduction of gp120-induced allodynia in EP3$^{-/-}$ mice by κ-opioid agonist. Gp120 (1 pg/mouse) was simultaneously injected with 5 pg of the opioid receptor agonist DAMGO (μ, ○, ●), DPDPE (δ, △, ▲), or U-50,488 (κ,□, ■) into EP3$^{+/+}$ (○, △, □) or EP3$^{-/-}$ (●, ▲, ■) mice. Assessment of allodynia was made as described in the legend for Fig. 1A. The value (mean ± SEM) represents the percent of the maximum possible cumulative score of 5–6 mice evaluated every 5 min.

(Fig. 7B) nor enhanced the [Ca^{2+}]i increase (100.7 ± 1.8% of HRP-gp120 alone, n = 61) in the cells that responded to HRP-gp120 (data not shown). In the second series of experiments with U-50,488, HRP-gp120 increased [Ca^{2+}]i in 406 cells (44.2%) out of 919 cells in spinal slices of EP3$^{-/-}$ mice. By the addition of U-50,488 (50 μM) to the perfusion solution, HRP-gp120 significantly enhanced the [Ca^{2+}]i increase (143.1 ± 6.0% of HRP-gp120 alone) in 277 cells (68.2%) of the gp120-responsive cells (Fig. 7C, left). Furthermore, as shown in Fig. 7C (right), U-50,488 (50 μM) induced a [Ca^{2+}]i increase in 34 cells (6.7%) out of 513 cells which did not show an increase in [Ca^{2+}]i induced by HRP-gp120 alone. In the third series of experiments, when the κ-opioid antagonist nor-BNI (50 μM) was included in the perfusion buffer, the [Ca^{2+}]i increase by HRP-gp120 was reduced to 117.6 ± 7.2% (n = 47) in 140 cells (33.6%) of the gp120-responsive cells, suggesting that the increase was mediated by the κ-opioid receptor.

4. Discussion

While the increase in [Ca^{2+}]i is known to be responsible for neuronal death by gp120 (Dreyer et al., 1990; Lannuzel et al., 1995; Medina et al., 1999), it has recently been suggested that PGE_2 production following the induction of COX-2, an inducible form of COX, is one of the possible mechanisms through which gp120 can cause neurotoxicity in the rat neocortex (Bagetta et al., 1998; Maccarrone et al., 1998, 2000; Corasaniti et al., 2000; Bezzi et al., 2001). In the present study, we demonstrated that gp120 induced mechanical allodynia in a dose-dependent manner, concomitant with a rapid and prominent rise in [Ca^{2+}]i in dorsal horn cells in the spinal cord. In agreement with previous reports (Harouse et al., 1991; Delézay et al., 1997), the galactocerebroside-mediated blockade of gp120 binding to spinal cells, of gp120-evoked allodynia, and of the [Ca^{2+}]i increase (Fig. 3C, 4B, and 5B) suggest that gp120 elicits its actions by binding to galactocerebroside on dorsal horn cells. Further, by the use of indomethacin and EP3$^{-/-}$ mice we obtained evidence suggesting functional connections of gp120 with the PGE receptor EP3 subtype and the κ-opioid receptor. The gp120-induced allodynia was blocked by pretreatment with indomethacin (Fig. 1A and C) and disappeared in EP3$^{-/-}$ mice (Fig. 2B). Pretreatment of spinal slices prepared from C57BL/6 mice with indomethacin also reduced the percentage of cells responsive to gp120 from 90.8 to 19.7% (Table 1), and a considerable portion of the indomethacin-treated cells showed increased [Ca^{2+}]i by the addition of the EP3

Table 1
Effect of pretreatment with indomethacin on [Ca^{2+}]i increase by gp120 in spinal cells

Pretreatment with indomethacin	Cells examined	Gp120-responsive cells	
		+ gp120[a]	+ gp120 +ONO-AE-248[b]
None	969	880 (90.8%)[c]	ND[d]
5 μM	234	211(90.2%)	8(0.3%)
10 μM	286	134 (46.8%)*	35(12.2%)
50 μM	407	80 (19.7%)*	99(24.3%)

[a] Number of cells with [Ca^{2+}]i increased by 2 nM HRP-gp120 alone.
[b] Number of cells with [Ca^{2+}]i increased by 2 nM HRP-gp120 in the presence of 10 μM ONO-AE-248.
[c] Data were analyzed by using a contingency table, and the Chi-square test was used as a post hoc test. *$P < 0.05$, as compared with HRP-gp120 alone group without indomethacin.
[d] ND, not determined.

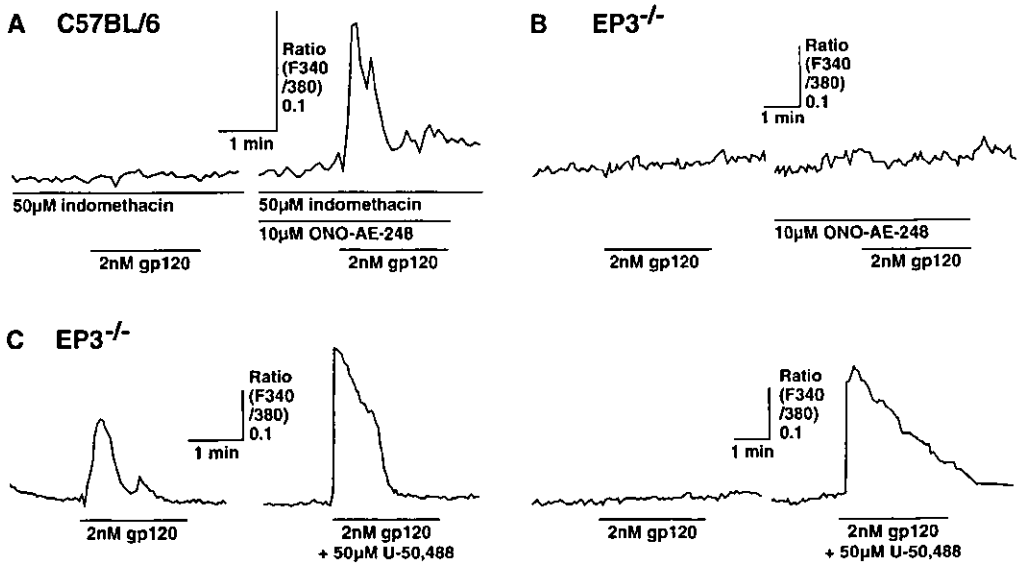

Fig. 7. $[Ca^{2+}]i$ changes caused by gp120 in spinal slices of C57BL/6 (A) and $EP3^{-/-}$ (B and C) mice. Spinal slices (A–C) were challenged with 2 nM HRP-gp120 followed by a second application of 2 nM HRP-gp120 + the indicated agent 25 min after the first application. The spinal slice in "A" was pretreated with 50 μM indomethacin for 3 h before the application of HRP-gp120. Time courses shown here are representative examples of typical $[Ca^{2+}]i$ responses in the spinal slice.

agonist ONO-AE-248 (Fig. 7A; Table 1). Compared with that of C57BL/6 mice, a much smaller percentage (31.9–44.2%) of cells responded to gp120 in the laminae III-VI of lumbar slices prepared from $EP3^{-/-}$ mice; and the $[Ca^{2+}]i$ response of these mice was not enhanced by ONO-AE-248 (Fig. 7B). Consistent with the reproduction of gp120-induced allodynia in $EP3^{-/-}$ mice by the treatment with the κ-opioid agonist U-50,488 (Fig. 6), this agonist enhanced the $[Ca^{2+}]i$ increase in 68.2% of gp120-responsive cells in spinal slices of $EP3^{-/-}$ mice and also induced $[Ca^{2+}]i$ increase in 6.7% of the cells that did not respond to gp120 (Fig. 7C). A recent study on spinally injured rats (Hao et al., 1998) supports our observation that U-50,488 did not alleviate the allodynic-like behavior, but rather enhanced it. Although the precise role of U-50,488 in gp120-induced allodynia in $EP3^{-/-}$ mice remains unknown, these results suggest that the site of action of the κ-opioid agonist is downstream of EP3 receptor activation. Since allodynia is induced within 5 min after *i.t.* injection of gp120 (Figs. 1 and 2), PGs, at least PGE_2, and an endogenous κ-opioid ligand, possibly dynorphin, mediate a rapid and prominent rise in $[Ca^{2+}]i$ in a group of dorsal horn cells in the spinal cord, which may be involved in gp120-induced allodynia. Fig. 8 shows a likely mechanism for the functional interaction of EP3 and κ-opioid pathways in induction of allodynia by gp120 in $EP3^{+/+}$ and $EP3^{-/-}$ mice.

The gp120-induced allodynia was insensitive to morphine (Fig. 1A), which characteristic is quite similar to that of allodynia induced by L5–L6 nerve ligation in rats (Plummer et al., 1992) or after peripheral nerve injury in humans (Fields, 1994). Consistent with these pain states, which are assumed to result from increased neuronal excitability and responsiveness known as the sensitization of wide dynamic range neurons in the deeper laminae (Woolf, 1994; Yaksh et al., 1999), cells in the deeper layer of the spinal cord were intensely stained with HRP-gp120 and showed an increase in $[Ca^{2+}]i$ in response to gp120 (Fig. 5). Spinal cord injured by compression produced biphasic eicosanoid production: an immediate phase attributable to COX-1, a constitutive form of COX, and a delayed phase attributable to COX-2; and the delayed synthesis of eicosanoids was suggested to be associated with the induction of COX-2 mediated by interleukin-1α (Totani et al., 1999). In analogy to these observations on spinal cord injury, *i.t.* gp120 might have evoked a biphasic PG production by COX-1 and COX-2 that leads to pain responses at an immediate phase and at a delayed phase. It was recently shown that *i.t.* gp 120 induced hyperalgesia and mechanical allodynia via the release of proinflammatory cytokines such as interleukin-1β and was suggested that activation of spinal cord microglia and astrocytes are critical for the effects of gp120 (Watkins and Maier, 1999; Milligan et al., 2000, 2001). In contrast to the reports on PG production by astrocytes in culture, immunoreactivity for COX-1 and COX-2 was found mainly in cell bodies and dendrites, but not axons or terminal fields, of neurons, structures that were typically postsynaptic (Breder et al., 1992, 1995). Whether PGs are released from neurons, from microglia, the cell type most frequently infected by HIV-1 in the central nervous system, or from astrocytes